J Supercond Nov Magn (2013) 26:593–617
DOI 10.1007/s10948-012-1800-1

ORIGINAL PAPER

A Microscopic Model of Superconductor Stability

Harald Reiss

Received: 19 October 2012 / Accepted: 14 November 2012 / Published online: 14 December 2012

Abstract The ratio $J_{\mathrm{Crit}}[T(x,y,t)]/J_{\mathrm{Crit}}[T(x,y,t_0)]$ of critical current densities (t_0 indicating start of a disturbance) integrated over sample cross section serves to calculate the "stability function", $\Phi(t)$, to predict under which conditions zero-loss transport current is possible. Critical current density and stability function are correlated with (conventional) timescale, t, in the superconductor (the "phonon aspect"). However, the stability problem is not simply restricted to coupled conduction/radiation heat transfer. It is questionable whether decay of electron pairs and subsequent recombination of excited electron states to a new dynamic equilibrium (the "electron aspect" under a disturbance) proceeds on the same timescale. A sequential model has been defined to calculate lifetimes of the excited electron states. These are estimated from analogy to the nucleon–nucleon, pion-mediated Yukawa interaction, from an aspect of the Racah-problem (expansion of an antisymmetric N-particle wave function from a $N-1$ parent state) and from the uncertainty principle, all in dependence of the local (transient) temperature field; with these approximations, the sequential model accounts for the retarded electron–phonon interaction. The numerical analysis is applied to NbTi and YBaCuO filaments in a standard matrix. As a result, the difference between both timescales can be significant, in particular near the phase transition: in the NbTi filament, a minimum distance of at least 60 μm (in this example) from the location of a disturbance should be observed for reliable stability analysis. This difference could have consequences also for safe operation of a resistive fault current limiter.

H. Reiss (✉)
Department of Physics, University of Wuerzburg, Am Hubland, 97074 Wuerzburg, Germany
e-mail: harald.reiss@physik.uni-wuerzburg.de

Keywords Superconductor · Dynamic equilibrium · Decay of excited states · Boson-mediated interaction · Retardation · Time-of-flight concept · Stability · Current limiter

1 Survey to the Stability Problem

A superconductor is stable if it does not quench under a disturbance, i.e., performs an undesirable phase transition from superconducting to normal conducting state. Disturbances comprise conductor movement, absorption of radiation, fault currents, or cooling failure. Disturbances frequently are transient, but there are also permanent disturbances like hysteretic losses. Stability models predict under which geometrical, thermal, and magnetic field conditions a transport current, during thermalization of the disturbance, will propagate without losses through the conductor. Traditionally, stability models rely on solely conduction heat transfer using analytical expressions; for a survey, see, e.g., Wilson [1] or Dresner [2]. Numerical investigations of the stability problem were presented, e.g., by Flik and Tien [3] and Reiss [4]. The impact of also radiation has been included only very recently [5].

Quenching proceeds on timescales, t, in the order of milliseconds or less. In standard stability analysis, decrease $dJ_{\mathrm{Crit}}[T(x,y,t>t_0)]/dt$ of critical current density (t_0 the time indicating start of the disturbance) during the corresponding warm-up period is considered to closely follow increase $dT(x,y,t)/dt$ of local temperature in the superconductor. Local temperature $T(x,y,t)$, usually measured with sensors thermally (mechanical or radiative) connected to the solid thus reflects the "*phonon* aspect" of the transient stability problem. In reality, superconductor stability is not confined to analysis of transient conduction/radiation heat

transfer. Instead, the question is whether decay of electron pairs, the "*electron* aspect" under a disturbance and subsequent recombination of excited electron states to a new dynamic equilibrium carrier concentration, proceeds on another timescale t' and whether *this* timescale is identical with the traditional (phononic) timescale, t.

Further, normal/superconductor phase transition during warm-up or cool-down periods traditionally is considered to occur at exactly the instant when solid temperature, $T(x, y, t)$, the output of the phonon aspect, coincides with critical temperature, T_{Crit}. Critical current density, $J_{\mathrm{Crit}}(x, y, t)$, under the assumption $t = t'$ then should become zero (or during cool-down return from zero to $J_{\mathrm{Crit}}(x, y, t) > 0$), exactly at this instant t. But it is not clear that during cool-down from normal conducting state, when at the time t, the temperature $T(x, y, t)$ becomes less than T_{Crit}, the previously normal conducting electron system of the superconductor has already completed return to a dynamic equilibrium mixture of normal conducting and superconducting components, in a two-fluid model.

Instead, at very low temperature, the superconducting electron system is decoupled from propagation of thermal waves. It reflects its own dynamic response to this or other specific excitations, by corresponding relaxation times, τ_{El} (in the following, we will call this time also a time constant, or a decay or average lifetime). Thermal diffusivity, on the other hand, determines a relaxation time, τ_{Ph}, for propagation of thermal (phonon) waves in solids after a thermal disturbance. Both relaxation times, τ_{El} and τ_{Ph}, after the same disturbance, are not necessarily identical; the lattice, if excited, behaves quite differently from the electron system.

A similar situation (two or more different relaxation times) arises in multifilamentary superconductors, again after a thermal disturbance: time constant, τ_B, for propagation of magnetic flux density, B, in the superconducting filaments is relatively small while thermal relaxation time, τ_{Ph}, is much larger, by orders of magnitude. The inverse of this relationship in the matrix material is of enormous importance for obtaining stability against quench in multifilament superconductors, in particular for high field applications.

In the present paper, lifetimes of thermally excited electron states are numerically calculated from their decay rates using a sequential model with contributions (a) from an analogy to an aspect of the nucleon–nucleon, pion-mediated Yukawa interaction, (b) from the Racah-problem (expansion of an antisymmetric N-particle wave function from an $N-1$ parent state; this aspect is to be observed in summations of individual decay widths to total lifetime, τ_{El}, of the excited electron system), and (c) from the uncertainty principle. The sequential model is designed to account for the retarded electron–electron interaction since the phonon mediating this interaction travels at finite speed. The model serves to estimate the time τ_{El} needed to reorganize the electron states to a new dynamic equilibrium that is described by an antisymmetric total wave function. Calculations are performed in dependence of transient temperature fields, $T(x, y, t)$, that are obtained from a rigorous finite element analysis. The analysis is applied to NbTi and YBaCuO filaments embedded in standard matrix materials.

The paper is organized as follows: in Sect. 2, a provisional comparison is made between thermal relaxation time, τ_{Ph}, and its electronic counterpart, τ_{El}; this is made to motivate investigation of the existence of, and relation between, the two timescales. Section 3 analyzes decay of excited electron states resulting from a thermal disturbance. Section 4 introduces details of the numerical calculations to extract lifetime, τ_{El}, of the excited electron system to define the timescale (roughly, $t' = t + \tau_{\mathrm{El}}$). Section 5 reports results for critical current density and stability function, and Sect. 6, in an example, shortly describes consequences of these results for operation and reliability of a resistive fault current limiter. Part of the description of the sequential decay model in Sects. 2 and 3 and in the Appendix A has been reported in [6], recently published by the author.

2 Provisional Estimates of τ_{Ph} and τ_{El}

At constant temperature, breaking of electron pairs and recombination can be described as a statistical process that establishes a dynamic equilibrium of the density of pairs and their decay products. Pair breaking and recombination proceed above a "Fermi sea" of single electrons that is unstable to even the weakest attractive electron–electron interactions between all electrons.

Because of the weak binding energy (some meV, correlated with an energy gap, $2\Delta E$, in the single-electron energy spectrum), electron pairs, besides statistical decay and recombination at constant temperature, are subject to also thermal excitations at any nonzero temperature. When $kT \ll 2\Delta E$ (k the Boltzmann constant), only few excitations will occur, and the electronic state is highly degenerate, otherwise the number of excitations may become large. Accordingly, after a sudden temperature increase, pair breaking will be observed before a new dynamic equilibrium is established at the increased temperature, and the new equilibrium is obtained after the relaxation time, τ_{El}, of the disturbed electron system, from recombination of the decay products to electron pairs.

As will be shown in this paper, mismatch between τ_{Ph} and τ_{El} occurs in particular near the phase transition. If this mismatch occurs, it will have significant impacts not only on critical current density and stability. Also onset or decay of persistent currents and results of experiments like levitation, or measurement of observables like electronic part of specific heat, or of thermal conductivity, can be affected.

We will in the following very generally speak of *elementary excitations* of the electron states if the superconductor

is below critical temperature (but not in the ground state), of *electrons* if single particle aspects in the superconductor are in the foreground (or if decay products from electron pairs are in normal conducting state), and of *quasi-particles* when collective electron aspects are considered.

Also (Bogoliubov) quasi-particles are elementary excitations in a superconductor. Properties of quasi-particles are similar to those of solid electrons if they reside near the Fermi level, which means that they can be assigned mass and momentum. They consist of a moving electron together with a surrounding exchange correlation hole, which means, in a pictorial description, that when an electron fights its way through a solid, other electrons must move out from its way, because of the Pauli exclusion principle, and to minimize the repulsive Coulomb energy. If the interaction between electrons is weak, all interactions that a single electron in a solid experiences can be renormalized into a self-energy state that defines the effective mass of a new particle, the quasi-particle. The original *many-body* problem among interacting particles that cannot be solved is, by renormalization, reduced to a *one-body* problem of free particles. For details, consult standard volumes on superconductivity; a picture describing quasi-particles in a superconductor that has become quite popular is presented by Mattuck [7], Chap. 1.

The special case of quasi-particles has to be taken into account when comparing the lifetimes of thermally initiated disturbances (as in the present paper) and disturbances initiated in current injection experiments. Though in both cases (thermal disturbances, current injection) decay of excitations proceeds by completely different mechanisms, comparison between both kinds of disturbances and their lifetime is illustrative: in current injection experiments, the decay of electron excitations is studied after an artificial increase of the number of *quasi-particles*. Instead, in the present case, we have an increase of the number of *excitations* if sample temperature, T, increases (while $T < T_{\mathrm{Crit}}$), with the total number of particles conserved. In current injection experiments reported, e.g., by Gray [8] or Epperlein et al. [9] in low temperature superconductors (LTSC; Al, Sn), thin films are used, with the injected electrical charge being collected in very thin surface layers, and data are taken at temperature far below T_{Crit}. Instead, here we investigate solid samples (filaments of NbTi and of YBaCuO) at temperatures close to T_{Crit}. Yet a provisional estimate of τ_{Ph} and τ_{El} can be made, even under these quite different experimental conditions.

Because Gray [8] or Epperlein et al. [9] applied thin films, for this provisional estimated, we also consider a thin film of $d = 100$ nm thickness onto the surface of which a very short thermal pulse (a "Dirac pulse" from a laser) is delivered (later, the analysis is focussed on filaments). Though the sample thickness in current injection experiments is definitely smaller than 100 nm, it is doubtful whether the following series expansion of rear sample surface temperature, $T(t)$, based on solely thermal conduction transport, would still be valid. For example, Al coatings evaporated onto thin 6 μm Mylar foils, with coating thickness below 50 nm, become transparent to radiation, and it is also questionable whether laser pulses short enough not to interfere with the thermal wave can be generated.

Assuming the thermal diffusivity, D_{th}, of the film is constant (independent of temperature), a series expansion of $T(t)$, see Carslaw and Jaeger [10], Chap. III, reads

$$T(t) = \sum b_n \sin\bigl[(n\pi x)/d\bigr] \exp\bigl(-D_{\mathrm{th}} n^2 \pi^2 t/d^2\bigr) \tag{1}$$

with expansion coefficients b_n and the summation in Eq. (1) over the index n taken from $n = 1$ to $n \to \infty$. If retaining only the $n = 1$ term and using for the diffusivity D_{th} of the film a value in the order of 5 m^2/s, typical for very pure (99.999 %) Al or Sn in their superconducting state, the thermal relaxation time, $\tau_{\mathrm{Ph}} = d^2/(D_{\mathrm{th}}\pi^2)$, would be several orders below 1 ns, and if film thickness is below 0.1 μm, as is the case in injection experiments, thermal relaxation would be completed even after much shorter periods of time. This value of τ_{Ph} is definitely smaller than τ_{El}, the lifetime of disturbed electron states, in the order of tens of microseconds, as is well known: such lifetimes have been observed in a variety of current injection experiments using Al or Sn films of about the same thickness or other materials like W or Ta under optical pulses.

Measurement of the quasi-particle recombination time (lifetime of the disturbed electron system) in superconducting Sn after injection of a current pulse was performed in [9] with current $i_P = 10.1$ mA and with the pulse duration $t_p = 1$ μs. There were about 6.3×10^{10} unit charges injected into a (total) volume of at least 3×10^{-14} m^3, which means an average of the injected particle density of about 2.1×10^{24} $1/\mathrm{m}^3$ (compare Fig. 3 in [9]).

Analogously, provisional estimate can be made for high-temperature superconductors (HTSC) like YBaCuO. During a thermal disturbance, the probability for exciting the electron system is proportional to $\exp[-\Delta E(T)/kT]$, under dynamic equilibrium conditions. Assume that a thin film HTSC sample of the same thickness as before (0.1 μm) is heated locally from 90.5 to 91.999 K (just below phase transition, $T_{\mathrm{Crit}} = 92$ K). With the electron density at temperatures close to absolute zero of about 6×10^{27} $1/\mathrm{m}^3$ of which a fraction of about $(\frac{1}{2})$ $(1/10)$ is available for pair formation, with the same (total) volume in which current was injected in [9], and using a standard (BSC) temperature dependence of $\Delta E(T)$ (see Eq. (24) in the Appendix A), this yields the number of thermally excited electron states (over the statistically generated number) of about 4.7×10^{26} $1/\mathrm{m}^3$. This number is by a factor M of about two orders of magnitude larger than in the current injection experiment (and still has to be considered as a lower limit).

A naïve order-of-magnitude estimate of the relaxation time τ_{El} in YBaCuO then can be made by assuming $\tau_{El,therm\ excit} \approx M\tau_{El,Current\ inject}$, with M the above constant and with $\tau_{El,Current\ inject}$ again in the order of 0.1 to 1 μs. This would result in a τ_{El} of at least 10 to 100 μs after a thermal disturbance in the HTSC, provided that the temperature is not too close to T_{Crit}. The result is much larger than the corresponding τ_{Ph}, here about 0.3 ns at $T = 90$ K using for YBaCuO the value of the diffusivity $D_{th} = 3.4 \times 10^{-6}$ m^2/s in Eq. (1), if again a Dirac pulse is applied to the film surface.

Diffusion length of quasi-particles is comparable to diffusion length of electrons, in low-temperature superconductors (LTSC) in the order of 10 to 100 μm at cryogenic temperature (e.g., 12 μm in Al at 14 K, see Table 44.1 in [11]). Diffusion length in HTSC is smaller, and thus we can safely assume that it can be neglected against sample dimensions in the experiments to be described in the following sections.

From the results of this provisional estimate of the two relaxation times it is quite interesting to investigate this problem in appropriate details. This is the aim of this paper.

3 Decay of Excited Electronic States

The superconducting state consists of two components that under (a) dynamic equilibrium or (b) nonequilibrium conditions, respectively, can be specified as follows:

(a) *After a purely statistical fluctuation, under strictly thermal equilibrium:* a super-fluid of electron pairs and a fluid of excited electron states, electrons or quasi-particles that exhibit some coherence behavior, both existing solely under statistical decay and recombination.
(b) *After a temperature increase (under a thermal disturbance) and before a new thermal equilibrium is established:* again a super-fluid of electron pairs and a fluid of excitations that now results solely from the temperature variation.

In both cases (a) and (b), the total number of solid particles is conserved. The situation is different from ordinary evaporation/condensation of conventional fluids, for example, a liquid with well-defined evaporation temperature and saturation vapor pressure: in superconductors, under a temperature variation well below critical temperature, contrary to evaporation/condensation in classical liquids, neither is there a measurable idle "background" (e.g., idle spectators consisting of excited electron states populated from decaying pairs and depopulated by recombination, both initiated spontaneously), nor will it be possible to simultaneously measure a dynamic "foreground", with a net decay rate of pairs after the end of a temperature increase, or a net condensation rate. Following a thermal disturbance, dynamic equilibrium state (a) exists only when the nonequilibrium state (b) has decayed completely until the next disturbance, and before this is accomplished, there is only one state, namely the predominant, nonequilibrium state (b) that can be observed in experiments and should be treated in the following analysis.

Generally, summation over the inverse of average lifetimes, τ_i, of the ith excited electron state, at a given constant temperature ($T > 0$), with the summation index, i, taken over all $1 \le i \le N_{Exc}$ (with N_{Exc} the number of thermal electron excitations), describes the decay rate (negative of the corresponding generation rate, G_{Exc}) at time t per unit volume:

$$G_{Exc}\big[T(t)\big] = (1/V)\sum\big\{1/\tau_{i,Exc}\big[T(t)\big]\big\}; \tag{2a}$$

dimension of $G_{Exc}[T(t)]$ accordingly is [1/(m^3 s)].

Dynamic equilibrium between electron pairs and their excitations exists and is described by Eq. (2a) if after having obtained equilibrium, recombination of excited electron states to electron pairs on the statistical average compensates decay, and vice versa. Equation (2a) essentially is identical to Eq. (3) in [8]; only a dependence on time of temperature, $T(t)$, has been added. At constant temperature, the rate $G_{Exc}[T(t)]$ on the time average is constant.

Equation (2a) can be written also in terms of decay widths, Γ,

$$G_{Exc}\big[T(t)\big] = (1/V)\sum\big\{\Gamma_{i,Exc}\big[T(t)\big]\big\}/(h/2\pi) \tag{2b}$$

of statistically or of thermally excited states, with the usual definition $\Gamma_i = (h/2\pi)/\tau_i$ and the summation index $1 \le i \le N_{Exc}$ of the excited electron states (h denotes the Planck constant). Advantages resulting from use of decay widths will later become obvious.

3.1 Thermal Disturbance of an Equilibrium and Subsequent Decay of Nonequilibrium States

Thermal equilibrium is displaced if, at a time t_0, temperature is suddenly increased to $T_1 = T + \Delta T$, still with $T_1 < T_{Crit}$. Assume that the temperature increase is initiated by local absorption of a short heat pulse. More electron pairs will decay (more than observed under dynamic equilibrium), and the positive generation rate, $G_{Exc}[T(t)]$, of excited electron states accordingly increases. After the end of the pulse, at time t_1, now the *disturbed* system decays, with negative generation rate $G_{El}[T(t)] = -G_{Exc}[T(t)]$, and after a time t_2 returns to a new dynamic equilibrium, where we observe, at the new temperature, $T(t_2)$, new constant (on time average) but dynamic decay and generation rates of electron pairs.

If under dynamic equilibrium a total wave function, $\psi(t_0)$, or a set of individual wave functions, $\phi_i(t_0)$, of which $\psi(t_0)$ is appropriately composed, describes the superconducting quantum state at the original time t_0, a thermal disturbance requires the *whole* set of the $\phi_i(t_0)$, not only part of

them, to be rearranged to a new total wave function, $\psi(t_1)$, at the end of the disturbance. As is the subject of this paper, $\psi(t_1)$ subsequently has to be rearranged to $\psi(t_2)$ because of decay of the excited state $\psi(t_1)$. The difference, $t_2 - t_1$, then is the lifetime, τ_{El}, of the disturbed electron states.

For rearrangement to the new total wave function, i.e., the procedure running from $\psi(t_1)$ to obtain $\psi(t_2)$, emphasis is on the *whole* set of the $\phi_i(t)$, not only part of them, that has to be taken into account. The situation is an analogue to calculation of "coefficients of fractional parentage" in atomic and nuclear physics (Mayer–Kuckuk [12], pp. 210–211, and references cited therein): if the antisymmetric, total wave function of a nuclear state incorporating N of nucleons shall be formulated, it can formally be expressed by appropriate coupling of an antisymmetric wave function of $(N-1)$ nucleons with a one-particle wave function. This yields the product

$$\psi\big((N-1), I, \alpha\big) \times \phi_i(j) \tag{3}$$

with I and j indicating angular momenta and the symbol α summarizing other quantum states to identify the $(N-1)$- and 1-particle configurations, respectively. But this wave function still has to be antisymmetrized. For this purpose, the wave function of the N-particle state will be expanded as a product of antisymmetric wave functions of $(N-1)$-particle states. In this expansion, addition of the one-particle state then requires rearrangement of *all* previous $N-1$ states to correctly obtain the new wave function, $\psi(t_2)$, that has to fulfill the Pauli exclusion principle; the corresponding expansion coefficients are the well-known Racah-coefficients. We are not interested in the exact formulation of the wave functions $\psi(t_1)$ and $\psi(t_2)$, but have to take into account all contributions to decay time, τ_{El}, that quite analogously to the Racah-problem result from reordering of the whole set of all particles involved in the antisymmetrizing procedure, from $\psi(t_1)$ to $\psi(t_2)$. After end of the disturbance, this concerns the constituents of still existing electron pairs plus the excited electrons.

In an ensemble consisting of an arbitrary number N of *any* kind of particles (not only excited electron states) that have to be reordered, after a disturbance from their corresponding equilibrium state, rearrangement of the total wave function then cannot proceed instantaneously (this is well known and will become also obvious for the superconductor in the following), but requires a time interval, the total lifetime $\tau = (t_2 - t_1) > 0$, of the disturbed system, before it has completed its return to dynamic equilibrium. Regardless in which manner reordering proceeds, the rearrangement rate, on the average, will be proportional to the ratio N/τ_{El}. In this paper, we will consider rearrangement (decay) of the excited states under two different points of view: decay proceeds in time and in space.

Assume that a local disturbance (a temperature increase) occurs at a particular position $\mathbf{x}'$ in the superconductor solid and at a time, t_0 (bold symbols denote vector quantities). At $t_1 > t_0$, we accordingly have at this position an increased concentration, $c(\mathbf{x}, t)$, of excited electron states over the previous equilibrium value.

The picture "decay in space and in time" then simply follows from the variation of the concentration $c(\mathbf{x}, t)$

$$dc(\mathbf{x}, t)/dt = \big(\partial c(\mathbf{x}, t)/\partial x\big)(\partial x/\partial t) + \partial c/\partial t, \tag{4}$$

which identifies the contributions "decay in space" $= (\partial c(\mathbf{x}, t)/\partial x)(\partial x/\partial t)$ and "decay in time" $= \partial c(\mathbf{x}, t)/\partial t$.

Because of propagation of the thermal wave,

(1) Decay in space means that the increased concentration, $c(\mathbf{x}', t_1 > t_0)$, from any arbitrary position $\mathbf{x}'$ of excited states is distributed by a transport process to positions $\mathbf{x} \neq \mathbf{x}'$; a particular simple transport mechanism is diffusion.

Application of the usual diffusion approach requires a definition of a corresponding mean free path of a stepwise (in space) propagating process that must be small compared to the sample dimensions. The final (stagnation) result will be $c(\mathbf{x}, t_\infty) > c(\mathbf{x}', t_0)$ for all positions $\mathbf{x}$ (including $\mathbf{x}'$) after a sufficiently long period of time, t_∞.

Rearrangement of the total wave function of the superconducting state cannot be completed before the disturbance (surplus number of excited state) has decayed completely to the concentration $c(\mathbf{x}, t_2 > t_1)$. Otherwise, rearrangement would lead to local surplus concentrations that again would have to be depopulated by subsequent diffusion steps.

(2) Decay in *time* means that the disturbed total wave function, $\psi(\mathbf{x}, t > t_0)$, that describes all electron states returns to equilibrium shape by recombination processes, with the stagnation result $\psi(\mathbf{x}, t_2)$. Thus decay in time means rearrangement of the total wave function by an operation that models recombination and transforms the total wave function from $\psi(\mathbf{x}, t > t_0)$ to its stagnation value, $\psi(\mathbf{x}, t_2)$, identical for all $\mathbf{x}$.

Contributions from both items (1) and (2) have to be summed up to lifetime, $\tau = \tau_{\mathrm{El}}$, of the disturbed system.

In the present paper, we will concentrate on only the second item, decay in time (see next sections), because this contribution is much larger than the contribution from item (1), decay in space, and it is thus already sufficient to demonstrate the magnitude of the difference, if any, between the two timescales, t and t'. Calculation steps for item (1) will be described in the Appendix A.

A general method to calculate lifetimes is provided by elements of perturbation theory, with operators describing

recombination of single particles to pairs, but (a) this procedure would require a large number of repeated applications, and (b) perturbation theory breaks down near phase transitions. Mattuck [7], Chap. 15, explains why the only way of handling retardation is to treat the mediating phonons field-theoretically, from the very beginning of an analysis. An alternative perhaps is time-dependent Ginzburg–Landau theory of the order parameter. In both cases, the computational effort is enormous due to the very complicated structure of the wave functions, each comprising components of a very large number of particles involved. Instead, we will use in Sect. 4 for item (2) an aspect of the Yukawa model of nucleon–nucleon interaction: a "time-of-flight" concept with a mediating Boson, considered as an analogue that can be used (with some caution, compare Sect. 3.2.3) to describe binding of two electrons to a pair in a superconductor.

While statistical fluctuations like those around the initial dynamic equilibrium concentrations are superimposed on the proper decay process (initiated by the thermal disturbance), they cannot substantially alter decay of disturbed states. This is explained by the mere existence of persistent currents of constant magnitude in superconductors: if there were very strong fluctuations, they would not be "statistical", which means that there would be no constant persistent currents at all.

For item (2), decay in time, and by practical reasons, the recombination of excited electron states to electron pairs is divided into two contributions (2a and 2b, compare Sects. 3.2.1 and 3.2.4) when calculating intrinsic decay widths Γ and lifetimes τ:

(2a) Contributions Γ_{ij} for two arbitrary particles i and j that determine an "intrinsic lifetime" of the nonequilibrium state. This contribution results from "correlation" efforts, a first step to be taken for recombination of particles i and j of a very large number, N. It requires a finite (though tiny) time interval needed before the proper condensation or recombination event to a pair can take place. "Correlation" in the sense used here strictly speaking means exchange of "information" between two quantum states; in reality it is the exchange of phonons that mediate binding interaction between single particles and that have to travel a nonzero distance between the particles concerned.

The basic question is whether in principle an *immediate* response of the electron system to a thermal disturbance or during recombination, or an immediate interaction between two particles, could be possible and the decay time, τ, simply be zero. With finite distances between particles to be correlated, this is certainly not fulfilled (exchange of phonons proceeds with rather limited speed), apart from conclusions from the uncertainty principle (the electron–electron interaction, accordingly, is retarded).

(2b) Contributions $\Gamma_{\mathrm{Rec}} = (h/2\pi)/\tau$ resulting from the uncertainty principle, for the proper condensation (or recombination) event, once the particles i and j are correlated (identified) in step (2a) that generates one pair from recombination of two, then correlated, particles i and j.

For recombination to *one* electron pair, each of the individual decay widths, Γ_{ij}, and Γ_{Rec}, of the excited electron state contributes by about 10^{-12} and 10^{-14} s, respectively, to individual lifetimes τ_{ij}, for an energy gap of some tens of meV. While these are very small contributions to total τ, there is a very large number of individual Γ_{ij}, and Γ_{Rec}, and correspondingly τ_{ij}, that have to be taken into account so that the total lifetime, τ, of the total disturbed state (the time needed to rearrange the total wave function) may become large, in particular near the phase transition; this will be shown later.

Because of the Pauli exclusion principle (and again in view of the Racah-problem), calculation of total lifetime, τ, from the two contributions (2a) and (2b) has to proceed in a stepwise manner; we will later call this procedure a "sequential model" (Sect. 3.3).

3.2 Decay in Time

The two contributions (2a) and (2b) to item (2) will now be estimated to find the individual lifetimes, τ_{ij}. We start with the contribution (2a) applied to arbitrary particles i and j (excited electrons, as decay products from any previously existing electron pair).

3.2.1 Estimate of the Contribution Γ_{ij} (Step 2a to Item 2)

For this approach, averages of the lifetime must be taken over a (virtual) volume V_C at all positions $\mathbf{x}$. It is clear that determination of the size of V_C may become one of the critical points of the analysis: on the one hand, we have to confine calculation of the average to small volumes, otherwise the number of particles concerned would be too large to be reasonably handled with numerical methods; on the other hand, an arbitrary dependence of the final results on size of V_C must be avoided. In the following, we will first estimate V_C.

3.2.2 Estimate of the Virtual Volume V_C

Two arbitrary electrons cannot have exactly the same wave function, because of the Pauli exclusion principle. If electrons could be considered as purely classical particles (point masses), with no interactions among each other, they all would statistically be independent, and the probability of finding an electron at a position $\mathbf{x}_j$ near an electron at a given

position $\mathbf{x}_i$ would be the same as for finding an electron at any position $\mathbf{x}_j$. This is not the case in a superconductor or, generally, if the Pauli exclusion principle is to be followed.

In the ground state (gs), the total wave function, with particles i and j counted by numbering $1, 2, 3, \ldots, N$, reads (compare standard volumes on superconductivity, e.g., Annett [13], Chap. 13, for an introduction)

$$\Psi_{\mathrm{gs}} = C \sum (-1)^P P\big[\phi(1,2)\phi(3,4)\phi(5,6) \cdots \phi(N-1)\phi(N)\big] \tag{5a}$$

with the summation extended over all $N!$ permutations, P, of the total number, N, of particles and zero center of mass motion. All pair wave functions, $\phi(i, j)$, must be antisymmetric with respect to exchange of particles i and j.

As usual, each of the $\phi(i, j)$ is written as a product of a symmetric space dependent part, $\phi_S(i, j)$, and of an antisymmetric, spin dependent part, $\chi_A(i, j)$. To determine the distance, $d = r_i - r_j$, between two arbitrary electrons i and j, we in principle need expectation values of the space part, $\phi_S(i, j)$, that describes the charge distribution of particles i and j. In a particularly simple picture, the $\phi_S(i, j)$ are expanded in terms of Bloch waves each of which is a free-electron plane wave,

$$\phi_S(i, j) = \sum a_k \exp\big[ik(x_i - x_j)\big], \tag{5b}$$

for description of s-wave states. This can be generalized to functions $f(|x_i - x_j|)Y_{lm}(\theta, \eta)$, with inclusion of direction of the vector $(\mathbf{x}_i - \mathbf{x}_j)$, but we need in the following only the distances, $|(\mathbf{x}_i - \mathbf{x}_j)|$.

For a description of excited states, instead of a transforming Ψ_{gs} (Eq. (5a)) to a total wave function, $\Psi_{\mathrm{Exc}} = \Psi(t_1)$, the BCS model starts with creation and destruction operators acting on the vacuum and in the following on the ground state. If just one electron pair is broken into two electrons, they have momentum vectors $\mathbf{k}'$ and $\mathbf{k}''$. With uncorrelated electrons, there is no electron with exactly $\mathbf{k}'' = -\mathbf{k}'$. Indication of spin-up or spin-down is omitted for simplicity. In the BCS-model (compare, e.g., Blatt [14], pp. 174–180, or again [13], Chap. 6), the total wave functions of ground and excited states, in terms of creation and destruction operators, read

$$\Psi_{\mathrm{gs}} = \Psi(t_0) = \Big[\prod \big(u_k + v_k b_k^+\big)\Big]|0\rangle, \tag{6a}$$

$$\Psi_{\mathrm{exc}} = \Big[\prod \big(u_k + v_k b_k^+\big)\Big] a_{k',+}^+ a_{k'',-}^+ |0\rangle, \tag{6b}$$

with probability amplitudes u_k and v_k to find the corresponding k-correlated pairs: for each broken electron pair, the k-pairs in the BCS-picture consist of two quasi-particles, one state unoccupied and the other occupied, respectively (the missing electron with momentum $\mathbf{k}'' = -\mathbf{k}'$ is represented by the "unoccupied" state). Creation and destruction operators are denoted by a_k and b_k, one for each index, k, and the index runs over all $k \neq k', k''$. The vacuum state is denoted by $|0\rangle$.

The operators $a_{k',+}^+$, $a_{k'',-}^+$ in Eqs. (6a), (6b) do not alter the functional dependence of the $\phi_S(i, j)$ on particle–particle distance (this does not imply that the distances are the same as before the excitation). While wave functions for central potentials are tabulated, centers of mass positions, r_i, r_j, cannot be calculated using the corresponding $|\phi_S(i, j)|^2$: because of symmetry of the $\phi_S(i, j)$, the results would be identical. Wave functions for other than central potentials are difficult to handle. An alternative is to directly estimate distances, without explicit recourse to wave functions, and this is made in the following.

To determine V_C, assuming a spherical volume, we need its radius, r_C. A first, direct but very rough estimate for the ground state can be performed using the interparticle distances, $d = (V/N)^{1/3}$, with N the number of particles filling a sample volume, V. With the inverse of the electron density in high-temperature superconductors ($\rho_{\mathrm{El}} = 6 \times 10^{27}$ 1/m^3), this yields a mean distance, d_m, between any two (among all) electrons of about 0.55 nm, or when taking only that part of the electrons that condense to electron pairs, a fraction of (1/10) of the total number, the mean distance increases to about 1.2 nm. This is about the coherence length of an electron pair in the ab-plane of high temperature superconductors.

A similar result is obtained from consideration of the Coulomb interaction within a (spherical) cloud of volume, V_C, of a large number of electrons. The radius, r_C, of V_C shall be given by the condition that the Coulomb potential energy between two arbitrarily selected electrons i and j, E_C, is minimized and below the binding energy, $2\Delta E$, of a single electron pair. The Coulomb energy amounts to

$$E_C(r_C) = \chi e_i e_j/(4\pi\varepsilon_0 r_C) \leq 2\Delta E(T) \tag{7}$$

with e_i and e_j denoting electron charge and ε_0 the dielectric constant.

In metals, the effective Coulomb force is modified by screening. In the solid, the electrostatic (repulsive) Coulomb potential consists of (a) the repulsive interaction (interpreted as a mean field) and (b) the (attractive) positive ion charges in the solid. The two contributions are superimposed. In the simplest form, this can provisionally be simulated using a screening factor, χ, in Eq. (7) that essentially modifies the dielectric constant. Comparison with the Thomas–Fermi potential, as the classical example of a screened Coulomb potential, will be made below.

Pairing of electrons in conventional superconductors is by formation of highly symmetric, singlet s-waves of charge distribution ($\mathbf{S} = \mathbf{s}_1 + \mathbf{s}_2 = 0$, from $\mathbf{s}_1 = 1/2$, $\mathbf{s}_2 = -1/2$, and $\mathbf{L} = \mathbf{l}_1 + \mathbf{l}_2 = 0$, from $\mathbf{l}_1 = 0$ and $\mathbf{l}_2 = 0$), and the energy

gap is finite and isotropic around the Fermi surface, in the ground state.

Pairing of electrons in unconventional superconductors like YBaCuO, with $\mathbf{S} = 0$ and $\mathbf{L} = 2$, is identified by spins and angular momenta $\mathbf{s}_1 = 1/2$, $\mathbf{s}_2 = -1/2$, $\mathbf{l}_1 = 1$, and $\mathbf{l}_2 = 1$. The corresponding charge distributions can approach each other more closely than in the highly symmetric case $\mathbf{s}_1 = 1/2$, $\mathbf{s}_2 = -1/2$, $\mathbf{l}_1 = 0$, and $\mathbf{l}_2 = 0$ states. Also, the energy gap is nonuniform, with zeros in particular directions.

Accordingly, if we estimate r_C using Eq. (7), singlet s-waves of charge distribution cannot approach distances below r_C, which in turn means that the virtual sphere, V_C, of radius, r_C, roughly contains *only* $\mathbf{S} = 0$ and $\mathbf{L} = 2$ electron pairs (states with larger but even angular momentum, $\mathbf{L} = 4, 6, \ldots$, are not very probable because they would indicate too large a rotational energy). Accordingly, in this very rough approximation, almost all electrons, $N_{\mathrm{El}}(t_0) = (\frac{1}{2})(\rho_{\mathrm{El}} V_C)/10$, contained within the volume V_C do not belong to $\mathbf{S} = 0$, $\mathbf{L} = 0$ but to $\mathbf{S} = 0$, $\mathbf{L} = 2$ spin and angular momentum states. Crystal imperfections and impurities could lead to false, s-wave-*like* charge distributions (see [15]); this will be neglected by simply assuming perfect crystalline order and very clean materials in this study.

Positions x_i, x_j of particles i and j, in one dimension, at time $t \geq t_1$ are predicted in the following using random variables RND_i and RND_j, with $0 \leq \mathrm{RND}_{i,j} \leq 1$ applied to the r_C, which yields the random distance $d(t) = x_i(t) - x_j(t)$ of particles before condensation to electron pairs. Selection of a lower limit of $d(t)$ does not have significant influence on the final results (in the calculations for the HTSC case, the coherence length of YBaCuO in c-axis direction was assumed for this limit).

As an alternative, results can be obtained also using the Thomas–Fermi potential,

$$E_{\mathrm{TF}} = E_C(r_C) \exp(-r/r_{\mathrm{TF}}), \tag{8}$$

with $E_C(r_C)$ from Eq. (7), without the factor χ, and r_{TF} the scattering length. Literature values of r_{TF} are in the order of 0.5 nm.

As Blatt ([14], p. 212) explains, screening of the Coulomb field in the superconducting state of the sample does not differ much from screening in the normal state; accordingly, we will continue with the familiar, normal state expression, Eq. (7), or with Eq. (8).

3.2.3 *Analogue to Nucleon–Nucleon Exchange Interactions*

The second information needed to calculate total lifetime τ of the excited electron system concerns the Boson that mediates binding of two electrons to a pair, as the final state (all of which constitute the new dynamic equilibrium). As an initial approach, we consider a nucleon–nucleon interaction model (with some caution) as an analogue to binding between two electrons in an electron pair.

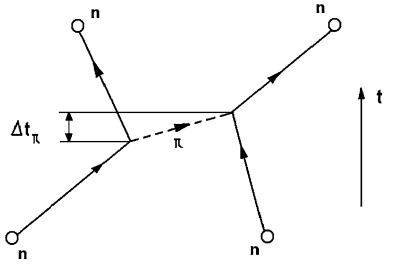

Fig. 1 Yukawa interaction between two nucleons (n) mediated by exchange of a pion (π, *dashed line*), as a particle system to which reference will be made in the text. The *arrow* on the *right side* denotes the direction of time, t

Nuclear forces (compare standard volumes on nuclear physics, e.g., again [12]) are short-range saturation forces. In the Yukawa model (Fig. 1), the pion (π), a Boson with spin zero, needs a time interval (in a rough picture a "time of flight") of about $\Delta t_\pi = 4.7 \times 10^{-24}$ s, much smaller than lifetime of charged pions (about 10^{-8} s), to mediate the binding energy between two nucleons. This time interval is estimated from the uncertainty principle using $\Delta E = m_\pi c^2$, with m_π the rest mass of the pion and c the velocity of light. It is not clear that its mass necessarily would be the rest mass of a free solid particle, but the range of the pion-mediated nuclear binding force (the "uncertainty of the nucleon radius"), $d = \Delta t_\pi c$, is about 1.4×10^{-15} m, a value surprisingly close to the radius of the nucleon.

In the deuteron, the only stable bound, two-particle nucleon system, we have a central binding force (plus a small electrical quadrupole moment) and a comparatively small binding energy so that the inter-particle distance between proton and neutron even exceeds the range of the nucleon–nucleon interaction force. This is in analogy to binding in the BCS-model: it is sufficient that there is a (negative) binding energy that even may be arbitrarily small.

There are of course differences between the three cases considered (nucleon–nucleon interaction, deuteron and electron pair): (a) in the deuteron, proton and neutron couple to a spin triplet ($^3S_1$)-state (parallel spins), and it is a free particle; (b) while the exchange Boson in the nucleon–nucleon interaction interacts between two solid particles, it does so only in the interior of a nucleus (we do not consider p–p or p–n scattering reactions); (c) in electron pairs of a superconductor, the exchange is between electrons, with the lattice vibrations that provide virtual Bosons to mediate exchange of energy and momentum.

But the other aspects of the electron pair formation, i.e., a two-particle interaction, a Boson (the phonon ω) as the (virtual) exchange particle and weakly bond, two-particle states, get the electron pair in superconductors, though only

from formal aspects, at least marginally similar to its nucleon/nucleon analogues. An alternative comparison could be made with the two-electron system in the ^{4}He-atom, but this comparison formally suffers from the central potential that the electrons in superconductors do not experience.

Formation of both a nucleonic bound state and of an electron bound state (the electron pair) in this model then would proceed within a time interval (the time of flight or lifetime, Δt_π or Δt_{ij}, respectively) that the corresponding exchange Boson (π or ω, respectively) needs to mediate the binding interaction (or *correlate* the corresponding single particles before recombination). After the time interval Δt_π, re-arrangement of the two single wave functions of the nucleons to a wave function describing a coupled state of two nucleons is accomplished, and Δt_π accordingly is the lifetime of two *uncoupled* nucleons considered as virtually disturbed states before they "condense" to a bound two-particle state in a nucleus. In the same way, Δt_{ij} is the time interval that is needed for recombination of two electrons to a pair and, when considering all Δt_{ij} and their appropriate summation, for rearrangement of the total wave function to describe the new dynamic equilibrium state obtained at time t_2.

The present model to estimate the contributions Γ_{ij} or Δt_{ij} in a superconductor to decay in time accordingly is based on the following analogy:

(1) In the Yukawa model, time of flight of the mediating Pion determines the uncertainty of the size of the *nucleon* (or the *lifetime* of two uncoupled nucleons before they combine to a nucleon–nucleon pair in a nucleus);
(2) In the electron pair, time of flight of the mediating Boson determines the uncertainty of the size of the *electron pair* (or the *lifetime* of two excited states before they recombine to an electron pair in a superconductor). The uncertainty of the size of the electron pair is the average "distance" between the two particles concerned.

In both cases, dividing this distance by the velocity of the corresponding exchange Boson, $d(t)/v_{\mathrm{Boson}}$, gives a measure for the "lifetime of the interaction" and, if appropriately summed up over all particles concerned, the intrinsic part of the "lifetime of the disturbance", $\tau = \tau_{\mathrm{El}}$, to be identified with the term $\partial c(\mathbf{x}, t)/\partial t$ in Eq. (4). This intrinsic lifetime concerns the disturbed state, not the proper existence of a pair; lifetime of a bound, two-particle system is of course different from this value (the deuteron is a stable particle, and without disturbances electron pairs in superconductors apart from statistical fluctuations on the average exist indefinitely, otherwise there would be no persistent currents).

3.2.4 Estimate of the Contribution Γ_{Rec} (2b to Item 2)

The estimate of this contribution is made according to an analogue to numerous examples reported in atomic, molecular, and nuclear physics in which decay of excited states is made by application of the uncertainty principle,

$$\Delta t_{1\mathrm{EP}} = (h/2\pi)/\Delta E_{1\mathrm{EP}}, \tag{9}$$

with the binding energy (the energy gap), $\Delta E_{1\mathrm{EP}}$. The time interval, $\Delta t_{1\mathrm{EP}}$, holds for decay of one electron pair (1 EP) to two excited electrons as well as for the present purpose, namely recombination of two excited electrons to one electron pair, or if an arbitrary large number of electron pairs are formed *instantaneously* from particles contained in the volume of the superconductor. With provisionally ΔE of 60 meV (at very low temperatures in HTSC), the contribution $\Delta t_{1\mathrm{EP}}$ amounts to about 10^{-14} s.

3.3 Sequential Model

Calculation of total lifetime, τ, requires contributions Δt_{ij} and $\Delta t_{1\mathrm{EP}}$ to be weighted by the number of allowed open decay channels. Weighing has to take into account the Pauli exclusion principle: only when rearranging the total wave function after creation of a new (recombined) pair (i, j) is completed, following this principle, the next re-arranging step can be allowed (this is an analogue to calculation of the coefficients of fractional parentage, compare Sect. 3.1). At a time t, this prevents formation of pairs $\phi(1, 2)$ and the corresponding total wave functions, ψ_{gs}, if at a previous time this pair would already have been formed, in any of the permutations in Eq. (5a). Formation of the total wave function, $\psi(t)$, cannot be completed before *each* permutation, $P[\phi(1,2)\phi(3,4)\phi(5,6)\cdots\phi(N-1)\phi(N)]$, contributing to the total sum is completed.

The maximum number N_{Cor} of possible correlations (two potential candidates suitable for building one pair) therefore is to be determined from a total of N_{Exc} particles by

$$N_{\mathrm{Cor}} = N_{\mathrm{Exc}}(t)!/\big[\big(N_{\mathrm{Exc}}(t) - 2\big)!2!\big]. \tag{10}$$

While the ratio $d(t)/v_{\mathrm{PH}}$ on the average determines the time needed for *one* correlation attempt, the total time for mediating the exchange energy between *all* potential candidates i and j to *one* electron pair (i, j) then is obtained by summation over all N_{Cor} *open* correlation steps to yield $\Delta t_{ij}(t)$, the time needed to rearrange the total wave function obtained by the recombination of particles i and j to the pair (i, j): the excited electron system will in the rearranging procedure not take just the very first from an arbitrary sequence of *all* potential combinations! The summation breaks up when for a particle, i, its appropriate particle partner, $j \neq i$, has been identified, to recombine to the pair (i, j); in the summation taken over a very large value of $N_{\mathrm{Exc}}(t)$ particles, we thus have on the average a factor of $\frac{1}{2}$ to be considered in the $\Delta t_{ij}(t)$.

Only when by this procedure the two electrons i and j properly are identified (by the conditions $\mathbf{s}_i = 1/2$,

$\mathbf{s}_j = -1/2$, $\mathbf{l}_i = 1$, $\mathbf{l}_j = 1$, and $\mathbf{p}_i = -\mathbf{p}_j$, namely at positions $x_i(t)$, $x_j(t)$ within V_C), the time interval $\Delta t_{1\mathrm{EP}}$ from Eq. (9) is added to $\Delta t_{ij}(t)$ to yield $\Delta t_{ij}^{\mathrm{rec}}(t) = \Delta t_{ij}(t) + \Delta t_{1\mathrm{EP}}$. This time interval incorporates correlation *and* recombination (index "rec") of two electrons to one pair, in terms of the total wave function, after one more electron pair has been added to the number of already existing pairs. After formation of a number N_{EP} of electron pairs, we have $N_{\mathrm{Exc}}(t) = N_{\mathrm{Exc}}(t_1) - 2N_{\mathrm{EP}}$ as the number of excitations to be used in Eq. (10) for the next selection of potential electron pairs, now from the reduced number $N_{\mathrm{Exc}}(t)$. This process is repeated until all N_{El} candidates (available in V_C) are coupled to pairs, which means that we have for the total time interval, $\Delta t^{\mathrm{total}}$, needed to accomplish rearrangement of the total wave function, a second summation,

$$\Delta t^{\mathrm{total}} = \sum \Delta t_{ij}^{\mathrm{rec}}(t), \tag{11}$$

with the summation index running over $2 \leq \Delta k \leq N_{\mathrm{Exc}}(t)$ in Eq. (11) using $\Delta k = 2$. It is clear that this procedure to calculate lifetime strongly differs from the balances given in Eqs. (8) and (9) of Ref. [8] that reflect a particle related picture to explain current injection experiments.

But computation time required to calculate the sum in Eq. (11) is enormous: for the HTSC, at $T = 90.5$ K, we have $N_{\mathrm{El}}(t_1)$ and N_{Cor} in V_C in the order of 10^4 and 10^8, respectively, which means that summations over a number of terms in the order of 10^{12} contributions would be the consequence. To simplify the procedure in such cases, instead of calculation of $d(t)$ from random positions x_i, x_j, we instead apply mean values, d_m, of the inter-particle distance, $d(t)$.

Distances, d_m, have been calculated for a value $\chi = 0.01$ of the screening factor (for numerical values of d_m obtained with an HTSC sample, compare [6]). It was found that the choice $\chi = 0.01$ sufficiently reproduces the results obtained with the Thomas–Fermi potential. When in the HTSC, temperature $T \to T_{\mathrm{Crit}}$ (92 K), all d_m diverge, due to the dependence of ΔE on T and thus of the radius r_C of the volume V_C in Eq. (7). This result is indeed the familiar one: all electron pairs finally decay into single, uncorrelated electrons as $T \to T_{\mathrm{Crit}}$. The divergence of d_m at temperatures close to T_{Crit} ($d_m > 10^{-6}$ m) yet should be interpreted as a tendency only, but it is clear that probability of decay of electron pairs increases as soon as the distance between both particles exceeds coherence length.

Note again that in this subsection we speak of "correlations", to identify potential partners for building a pair. In the traditional particle picture, particle–particle distances as $T \to T_{\mathrm{Crit}}$ become much larger than average electron distances in any normal conducting solid. There is no longer any interaction between two electrons separated by such distances (except for very exotic cases) that would be sufficient to build up pairs. In a superconductor and in the correlation picture used here, strongly increased d_m thus destroys correlation between two potential candidates. Accordingly, neither pairs can be formed, to overcompensate statistical decay/condensations events, nor do electron pairs any longer exist at all if $T \to T_{\mathrm{Crit}}$, and superconductivity breaks down.

In summary, the sequential model to determine lifetimes accordingly is based on

(a) the uncertainty principle to estimate the time interval needed for the proper (condensation-like) recombination or (evaporation-like) decay of a pair,
(b) the total wave function of excited states factorized into space components, $\Phi_S(i, j)$, of which solely the dependence on distance between arbitrary particles i and j out of a large multiple is considered here,
(c) a model to estimate the distance between particles i and j before recombination,
(d) an analogy between the phonon-mediated binding force between two electrons with the pion-mediated Yukawa nucleon–nucleon force (together with the "time-of-flight" concept), and
(e) the Pauli principle, which is reflected in a sequential model for the calculation of total lifetime, τ, of disturbed state.

But the situation still might be more complicated for more than only one reason. For example, de Gennes ([16], p. 99) reports that ion charges oscillating near the resonance frequency of thermal ionic motion could "over-screen" the negative charge of either electrons 1 or 2 in Eq. (7), or the mean field of all other electrons. As a consequence, the uncertainty of the estimate of d_m will increase, with corresponding uncertainties in the summation indices. We have to leave open this and other problems to another study.

Summarizing the contributions from diffusion (decay in space, Appendix A) and sequential model (decay in time), we have for the total lifetime near the phase transition, in a good approximation, $\tau \approx \tau_{\mathrm{El}} = \Delta t^{\mathrm{total}}$, because the contribution to τ from decay in space was found to be very small, at least for the HTSC case.

3.4 Decay Rates

Total conversion rate, from $N_{\mathrm{Exc}}(t > t_1)$ excited electrons located in the volume V_C to $N_{\mathrm{Exc}}(t)/2$ electron pairs, by application of the lifetimes, $\tau \approx \Delta t^{\mathrm{total}}$, estimated in the previous section, read

$$G_{\mathrm{Exc}}(t) = dN_{\mathrm{Exc}}/dt = N_{\mathrm{Exc}}(t)/\tau. \tag{12}$$

For temperature clearly below T_{Crit}, the total volume of the solid contains a very large number of single spherical cells, V_C, with the G_{Exc} in each cell being identical. This means that the decay rates G_{Exc} calculated in Eq. (12) per unit cell volume yield also the decay rates of the whole solid because decay will most probably, apart from differences resulting

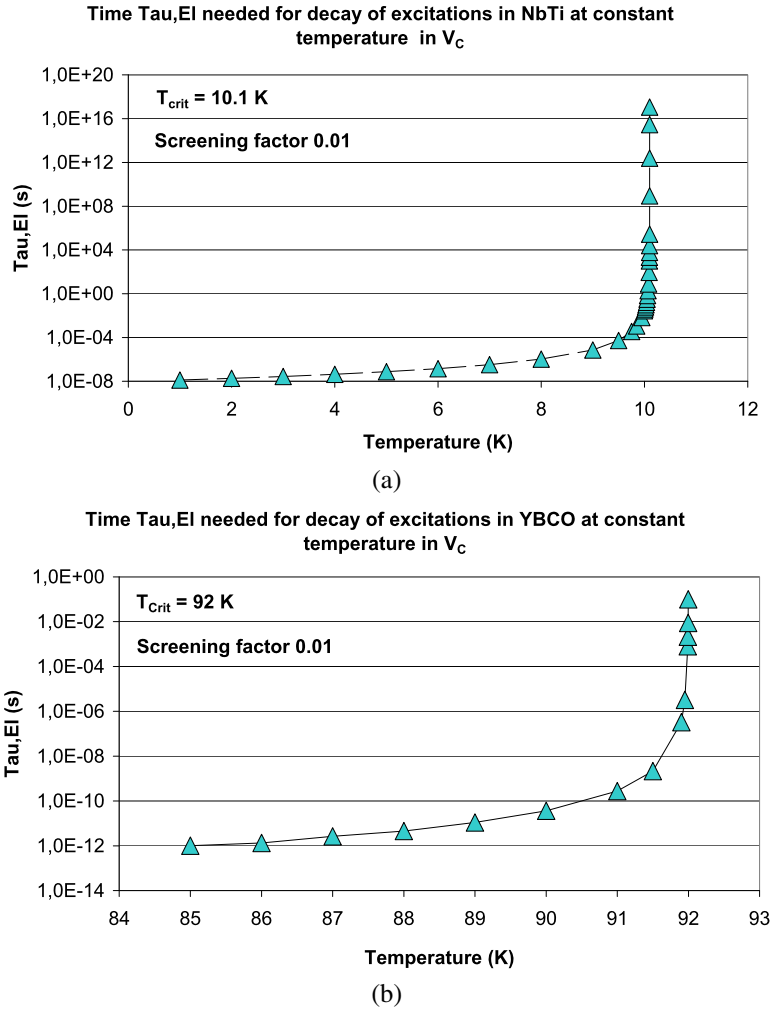

Fig. 2 (**a**) Time constant (relaxation time for decay, or average lifetime), τ_{El}, of excited electron states needed for decay of thermal excitations in a superconducting NbTi filament, calculated at constant temperature and using a screening factor, $\chi = 0.01$, to the Coulomb potential (Eq. (7)), in a virtual conductor volume, V_C (see text for more explanations). (**b**) Time constant, τ_{El}, for decay of thermally excited electron states in a virtual volume, V_C, of a superconducting YBaCuO filament. Compare the figure caption to (**a**) (Color figure online)

from variations of the temperature field, proceed in parallel in each cell. The decay rates depend on the volume V_C because $\Delta t^{\mathrm{total}}$ is calculated by means of the number of particles contained within this volume. The procedure thus relies strongly on the size of the cells, V_C, but the situation relaxes if temperature during warm-up converges to T_{Crit}. The distances, $d(t)$ or d_m, and thus the volume, V_C, increase strongly, which means that the V_C finally will fill the total sample volume. At a certain time, t, the distances $d(t)$ or d_m exceed sample dimensions. Then $G_{\mathrm{Exc}}(t) \to 0$, and dependence of $G_{\mathrm{Exc}}(t)$ on the size of V_C has disappeared. This means that the approximations used here will become the more appropriate the more the temperature in the cells approaches critical temperature.

Decay times, $\tau = \tau_{\mathrm{El}}$, that result from application of Eq. (12) are plotted in Fig. 2a, b vs. temperature (compare Sect. 4). The curves approach very large values as temperature $T \to T_{\mathrm{Crit}}$. The divergence of τ_{El} simply indicates the tendency of the system to approach dynamic thermal equilibrium, which at constant temperature is of quasi-infinite lifetime (again apart form statistical fluctuations). The τ in the temperature region very close to T_{Crit} accordingly indicates probabilities for stability of a certain electronic state. It is not possible to extend these calculations to exact T (constant) $= T_{\mathrm{Crit}}$: divergence resulting from the dependence on temperature of ΔE, see Eq. (24) in the Appendix A, is too strong to be handled numerically already if the temperature difference between T and T_{Crit} is below 10^{-6} K. In the extreme case $[T_{\mathrm{Crit}} - T\,(\mathrm{constant})] \to 0$, *with T constant*, it would take the superconductor indefinitely long time to allow recombination of all available excitations to pairs, again a natural consequence of the uncertainty principle: the case $T = T_{\mathrm{Crit}}$ (T constant) simply is the dynamic equilibrium of the electron state when no more disturbances, apart from statistical fluctuations, have to be compensated.

This result, increase of τ to indefinitely large values if $[T_{\mathrm{Crit}} - T\,(\mathrm{constant})] \to 0$, cannot be achieved if summations over contributions $d(t)/v_{\mathrm{Ph}}$ or d_m/v_{Ph} would be omitted and in total be replaced by constants. The same conclusion applies to the decay widths that for $T \to T_{\mathrm{Crit}}$ would not increase strongly without the summations over the N_{Cor} potentially open decay channels.

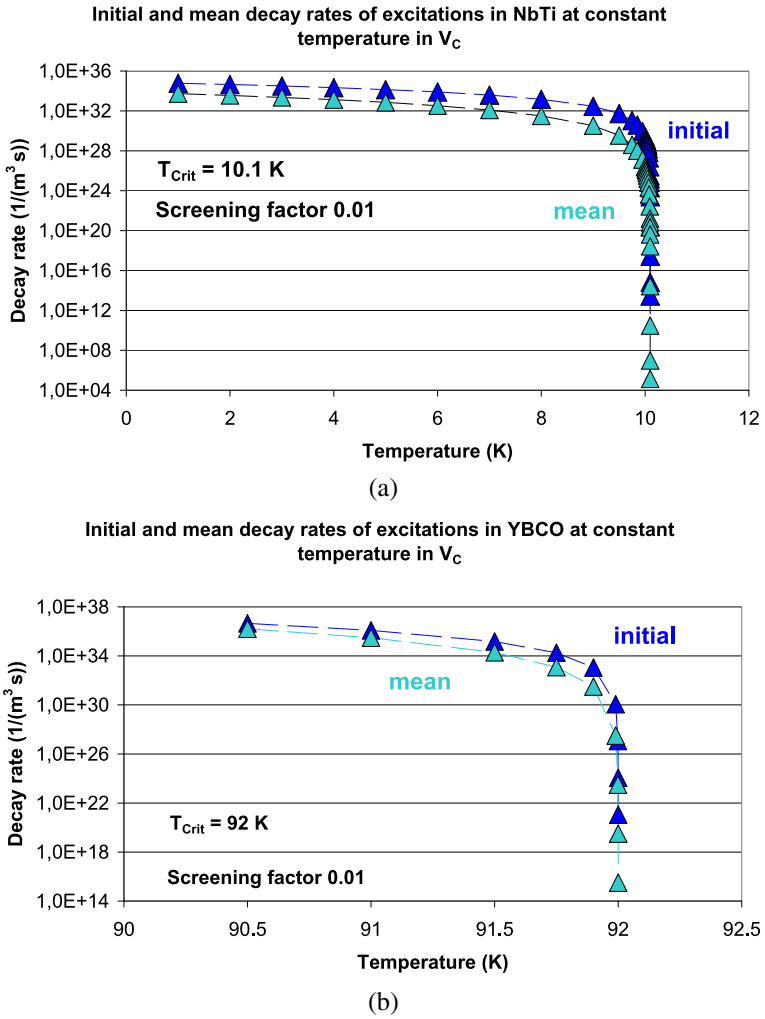

Fig. 3 (**a**) Initial and mean decay rates (per unit volume) of thermally excited electron states in the virtual conductor volume, V_C, calculated for the NbTi filament at constant temperature and for the same screening factor to the Coulomb potential as in Fig. 2a, b (see text for more explanations). (**b**) Initial and mean decay rates (per unit volume) calculated for the YBaCuO filament at constant temperature and for the same screening factor to the Coulomb potential as in Fig. 2a, b (see text for more explanations) (Color figure online)

But since warm-up *continues* and the temperature, $T(t)$, is not constant but increases, all quantities that depend on temperature like J_{Crit} and the stability function (and others, see Sect. 6), accordingly, are *not* constant, too, and this applies also to lifetimes, τ. Accordingly, we have to consider correction of "real" time, t (the standard timescale), to another timescale, see Sect. 4.3.

The decay rates decrease with increasing number of already existing electron pairs (from recombination of the decay products after the disturbance). We therefore can identify not only final (τ_{El}) but also initial and mean recombination rates, as has been done in Fig. 3a, b. Initial decay rates at temperatures close to T_{Crit} are much larger than the mean rates.

3.5 Comparison with Classical Exponential Decay Formula

As a conclusion of this section, we can compare the decay of the thermally excited electron states with the classical exponential decay formula. If $N_{\mathrm{Exc}}(t)$ denotes the number of excitations still existing after start of decay of the excited electron system after a thermal disturbance, in the classical picture we would have

$$N_{\mathrm{Exc}}(t)/N_{\mathrm{Exc}}(t=0) = \exp\bigl[-\lambda(T)\times t\bigr] \tag{13}$$

with a decay constant, $\lambda(T)$, that in the present model depends on temperature and time. This can be explained as follows: using $\Gamma(t) = (h/2\pi)\times\lambda(t)$, the decay of the excited states can be described by the decay width, $\Gamma(t)$, i.e. the probability for decay, that should *increase* as the number, $N_{\mathrm{Exc}}(t)$, approaches zero. This is different from classical, e.g., radioactive, decay: there, the probability of decay of instable nuclei is always constant, regardless how large the number of still existing nuclei, and so are λ and Γ. Here, the smaller $N_{\mathrm{Exc}}(t)$, the faster the decay of this number, and the larger the decay width or decay probability as time increases until decay is completed. If the number $N_{\mathrm{Exc}}(t)$ has already become small, for the still existing excitations (single electrons), it is "easier" to find suitable partners to form pairs, see below.

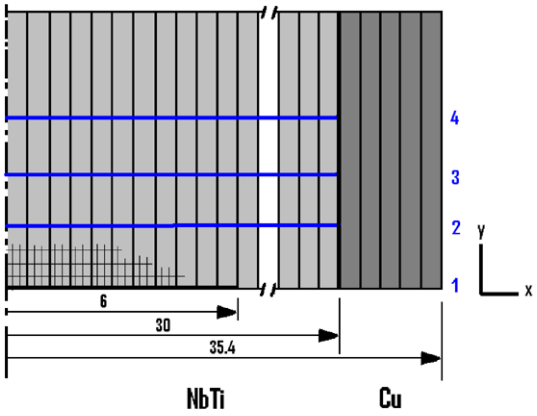

Fig. 4 Section of a superconductor filament (NbTi or YBaCuO) embedded in a matrix material (Cu or Ag, respectively). Schematic presentation (not to scale), under cylindrical symmetry (the *vertical dashed-dotted line* indicates axis of symmetry). All radii are given in micrometers. Superconductor and matrix material are identified by *light grey* and *dark grey shading*, respectively. The target area (of radius 6 μm) is indicated by the *horizontal thick black line*. *Horizontal blue lines* indicate planes 1 to 4 used for calculation of the stability function and of zero loss transport current in Figs. 10, 11, and 14 (compare text for definition), at different axial distances from the target area. The finite element mesh is schematically indicated by *thin horizontal* and *vertical lines* (Color figure online)

Using Eq. (13), with the number of still existing excitations, after start of decay of the thermal disturbance, we calculate in the usual way, from $LN[N_{\mathrm{Exc}}(t)/N_{\mathrm{Exc}}(t=0)]$, the decay constant $\lambda(t)$ and the decay width $\Gamma(t)$, compare Fig. 15 in [6] for YBaCuO, $T = 91.9$ K, and a screening factor $\chi = 0.01$ (if using other temperatures or screening factors, the qualitative behaviour $\Gamma(t)$ is the same).

As was expected, the decay width, or the probability of decay, increases with time as soon as $N_{\mathrm{Exc}}(t)$ approaches zero (compare Fig. 15 in [6] or Fig. 15 in Appendix B): if only few particles are left to recombine to pairs, completion of recombination or rearrangement of the total wave function proceeds the faster the smaller this number (particles i find their partner particles j more quickly), and the probability for decay accordingly increases.

This behavior, strong increase of the decay probability as $T \to T_{\mathrm{Crit}}$, would not be obtained without the correlation steps, i.e., the summations described in Sect. 3.3.

4 Details of the Numerical Calculations

4.1 Data Input to Finite Element Simulation

Figure 4 schematically shows a section of a cylindrical superconductor sample, a filament of 30 μm radius and of arbitrary length (in this example, at least 300 μm). The vertical dashed-dotted line indicates the axis of symmetry. The filament is embedded in a cylindrical, 5-μm-thick standard matrix material (here Cu; shaded region in Fig. 4; this means that, in a multifilament wire, each filament would be separated from its neighbors by at least 10 μm). A target spot (thick horizontal line at $y = 0$) indicates location of a disturbance. Radius of the target spot is $r_{\mathrm{Target}} = 6$ μm. Without loss of generality, the disturbance is modeled as a surface source; a disturbance occupying a finite volume could be designed as well. Because of symmetry, only the region $x \geq 0$ is modeled.

Calculations are performed for NbTi and YBaCuO filaments. One could argue that a radius of 30 μm could be rather large for NbTi filaments in a multifilament wire while it is difficult to produce high-quality YBaCuO filaments of this radius at extended conductor lengths. However, the overall results of this study will not be affected from this assumption.

At the axial position (or plane) $y = 0$ of the filament, a single heat pulse onto the NbTi and YBCO filaments of in total 2.5×10^{-10} or 3×10^{-8} W s, respectively, shall be distributed as a thermal disturbance of $\Delta t_P = 8$ ns duration; the pulse is uniformly distributed over the target radius. Because of symmetry, the light-grey shaded region experiences a heat pulse of half this value. The length Δt_P is the same as applied in [5, 6], and [17].

Like in [5, 6], and [18], for a first check of coincidence of the FE result with stagnation temperature, stagnation temperature, $T(\infty)$, was calculated using temperature-independent values of thermal conductivity, λ, and specific heat, c_p. Coincidence was found, at a time $t = 10^4$ s after start of the disturbance, at all internal positions of conductor volume; the maximum difference between both methods was in the order of 10^{-2} per cent. Isotropic conductivity and specific heat, mapped meshing, and time steps of at least 10^{-12} s were used in this initial finite element (FE) calculation. This procedure simply serves to check whether meshing and time steps appropriately were chosen for the strongly nonlinear finite element method.

But in all following calculations, λ and c_p are treated as temperature-dependent quantities; data for the NbTi filament and Cu are taken from various standard literature sources, data for the YBaCuO filament and Ag are the same as used in [5, 6], and [18]. Thermal conductivity in the following calculations also takes into account anisotropy of conductive heat transfer in YBaCuO, in directions parallel or perpendicular to the crystallographic ab-plane of this material (like in the mentioned references, an anisotropy factor of 10 has been applied in the calculations).

As a result, Fig. 5a, b shows calculated *nodal* temperature evolution, $T(x, y, t)$, at the central position of the target spot ($x = 0, y = 0$), at the periphery of the filament ($x = 30$ μm, $y = 0$), and, for the same x-positions, at an axial distance $y = 300$ μm from the target spot. Data are calculated for the thermal disturbance $Q = 2.5 \times 10^{-10}$ (NbTi) or 3×10^{-8} W s (YBaCuO). At the end of the disturbance,

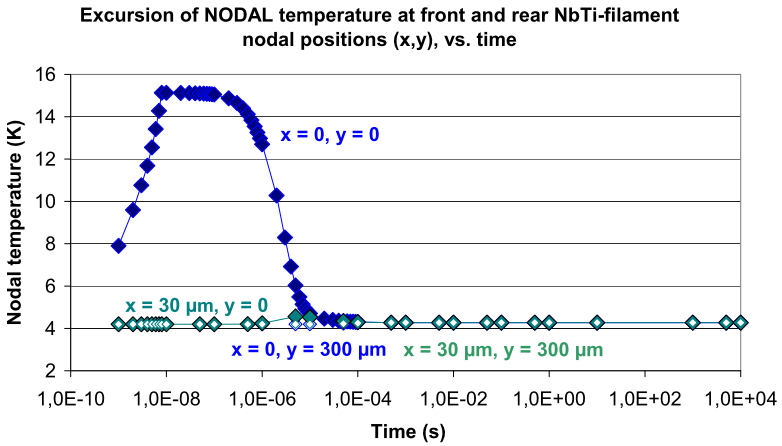

(a)

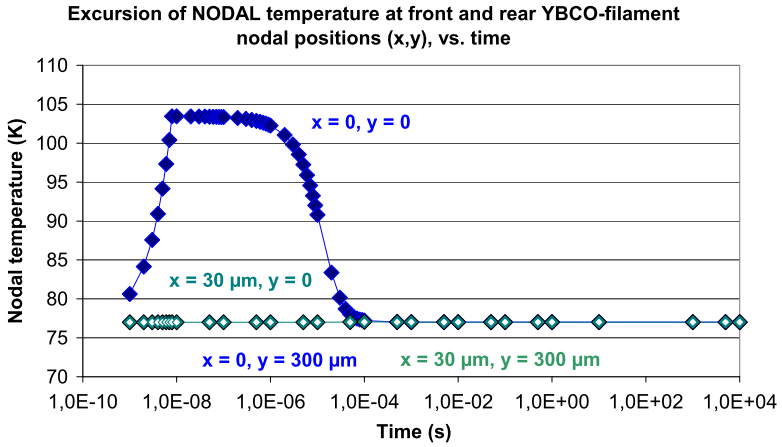

(b)

Fig. 5 (**a**) Nodal temperature, $T(x, y, t)$, obtained from a finite element simulation, at front ($x = 0$, $y = 0$) and rear positions ($x = 0$ or 30 µm, $y = 0$ and 300 µm, respectively) calculated for the superconducting NbTi filament under a heat pulse absorbed at radial positions $0 \le x \le 6$ µm, $y = 0$, of $Q = 2.5 \times 10^{-10}$ W s during a period of 8 ns. (**b**) Nodal temperature, $T(x, y, t)$, in the superconducting YBaCuO filament. Same finite element calculation as in (**a**), with absorption of a heat pulse of $Q = 3 \times 10^{-8}$ W s during 8 ns (Color figure online)

$t = 8$ ns, the nodal temperature at the position ($x = 0$, $y = 0$) indicates the maximum temperature that is obtained in the samples during the whole simulated period. Critical temperatures are 10.1 and 92 K for the NbTi and YBaCuO filaments, respectively. All curves $T(x, y, t)$ in Fig. 5a, b (and also temperatures at all other positions in the filaments and matrix materials) converge to their stagnation temperatures.

Figure 6a, b show NbTi and YBaCuO *element* temperatures calculated from the corresponding nodal values. Magnitudes of the thermal disturbances were chosen to yield maximum element temperatures close to but safely below T_{Crit} (this choice avoids divergence of the decay rates that would be observed if $T \to T_{\mathrm{Crit}}$ and the related numerical problems). At the axial distance $y = 300$ µm, there is hardly any observable increase of element temperature above start values (temperature of the coolants) that could be observed after end of the disturbance.

4.2 Critical Current Density

Different temperature fields must lead to different predictions of superconductor stability. This follows immediately from the temperature dependence of critical current density, J_{Crit}. This dependence provides a single-valued mapping of the temperature field $T(x, y, t)$ to the field $J_{\mathrm{Crit}}(x, y, t)$ of critical current densities if there is no magnetic field.

The temperature dependence of $J_{\mathrm{Crit}}(T)$ can be modeled as

$$J_{\mathrm{Crit}}(T) = J_{\mathrm{Crit}}(T = 0) \times [1 - T/T_{\mathrm{Crit}}]^n. \tag{14}$$

The theoretical Ginzburg–Landau value of the exponent n in Eq. (14) is 3/2. This exponent was used for the NbTi-filament calculations.

For the YBaCuO filament, experimental investigations show that the exponent neither is independent on the method of preparation (thin films, substrate and its microstructure, 1G and 2G wires?) nor is identical for all temperature regions below T_{Crit} (quantum creep, flux line core pinning, or thermally activated depinning regimes; see the discussion in [5] that will not be repeated here. The value $n = 2$ should approximately be applicable for the present purpose.

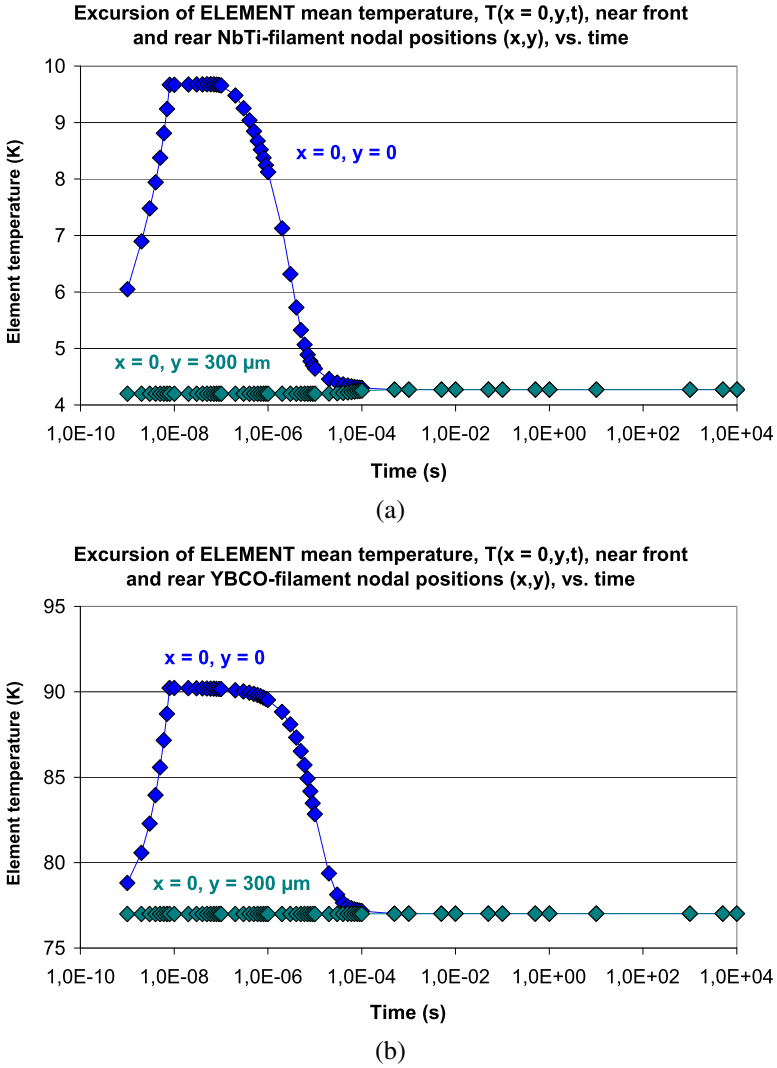

Fig. 6 (**a**) Element temperatures (elements in the finite element scheme, Fig. 4) in the NbTi filament calculated for elements located near front and rear nodal positions from the nodal temperatures in Fig. 5a. (**b**) Element temperatures in the YBaCuO filament. Same calculation as in (**a**) (Color figure online)

Assuming $J_{\mathrm{Crit}}(x, y, t = 0) = J_{\mathrm{Crit}}(T = 4.2\ \mathrm{K}) = 7 \times 10^5$ A/cm^2 of NbTi and $J_{\mathrm{Crit}}(x, y, t = 0) = J_{\mathrm{Crit}}(T = 77\ \mathrm{K}) = 10^5$ A/cm^2 of YBaCuO in zero magnetic field, this fixes the corresponding $J_{\mathrm{Crit}}(T = 0)$.

Accordingly, at positions close to the target spot, J_{Crit} will become small in both cases, but the larger the axial distance (and the larger time t), the larger J_{Crit}, in strict correspondence to the behavior of the transient temperature field, $T(x, y, t)$.

Using Eq. (14), Fig. 7a, b shows critical current density $J_{\mathrm{Crit}}(x = 0, y, t)$ calculated for the NbTi and YBaCuO filaments from the corresponding element temperatures (Fig. 6a, b). Since there is hardly any temperature increase at positions ($x, y = 300$ µm), the critical current densities are not affected at these positions, at all times t. The stability functions that result from these distributions of critical current density accordingly will be close to zero at these positions (Sect. 5).

4.3 Numerical Estimate of Lifetimes

Following Eqs. (10)–(12), results for decay rates and lifetimes of thermally excited electron states in NbTi and YBaCuO correspond to constant temperature. In order to correctly reflect increasing sample temperature during the disturbance, lifetimes have to be transformed to values t', the internal timescale. Time dependency of lifetime has to reflect the temperature dependency, $d\tau_{\mathrm{El}}/dT$, of lifetime, τ_{El}, and the time dependency, dT/dt, of the corresponding temperature fields, $T = T(x, y, t)$. Real time t thus is shifted, from timescale t to timescale t', by $t' = t + \Delta t'$, using for the time shift $\Delta t'$ the quantity

$$\Delta t' = \tau_{\mathrm{El}} = (d\tau_{\mathrm{El}}/dT)(dT/dt)\Delta t. \tag{15}$$

In Eq. (15), the first and second factors (derivative of τ_{El} with respect to temperature and derivative of temperature

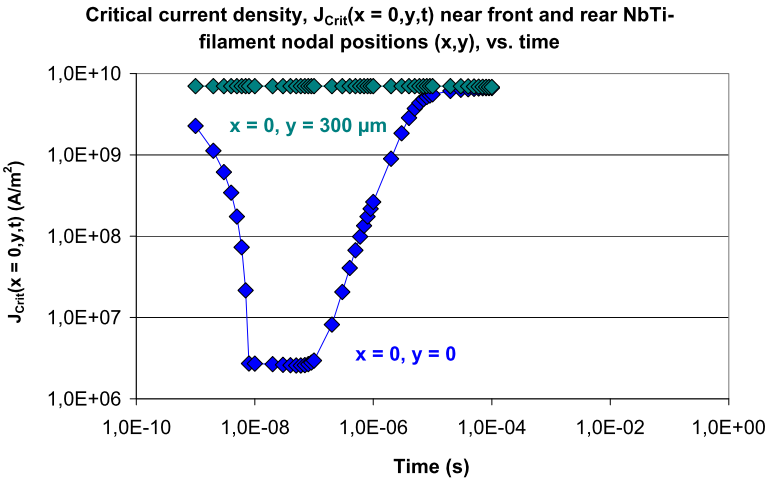

(a)

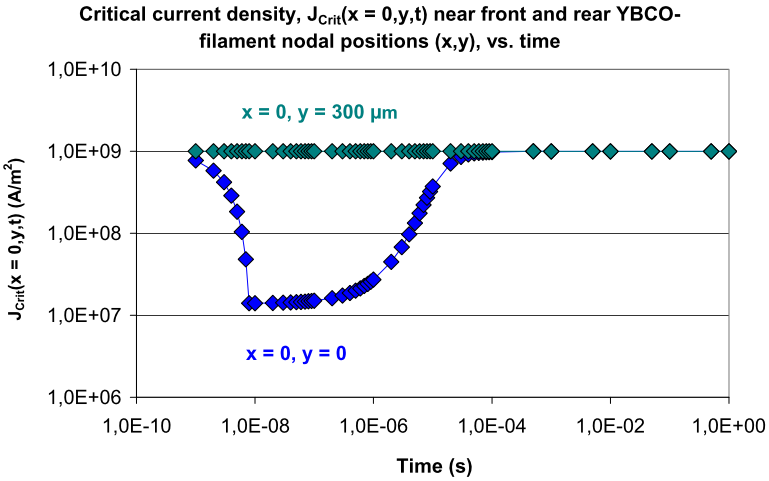

(b)

Fig. 7 (**a**) Critical current density in elements located near front and rear nodal positions in the NbTi filament calculated using Eq. (14) with the exponent $n = 3/2$ from the element temperatures reported in Fig. 6a. (**b**) Critical current density in elements of the YBaCuO filament calculated using Eq. (14) with the exponent $n = 2$. Same calculation as in (**a**) (Color figure online)

field with real time) are obtained from Figs. 8a, b and 9a, b, respectively.

The stability function, $\Phi(t)$, then can be plotted vs. time in the real time scale, t, and for comparison vs. time in the alternative "shifted" timescale, t', as explained in the next section.

5 Results for the Stability Function

We will first explain the standard definition of the stability function, $\Phi(t)$, in dependence of real time t.

5.1 Conventional Presentation of $\Phi(t)$ on the Timescale t

The stability function applies the ratio $J_{\mathrm{Crit}}(x, y, t)/J_{\mathrm{Crit}}(x, y, t = 0)$ of transient critical current densities to critical current density at $t = 0$

$$0 \le \Phi(t) = 1 - (1/A) \int \big(J_{\mathrm{Crit}}(x, y, t)/J_{\mathrm{Crit}}(x, y, t = 0)\big) dA \le 1 \tag{16}$$

with the integral taken over the conductor cross section, A, at an axial position (plane), $y \ge 0$. The ratio $J_{\mathrm{Crit}}(x, y, t)/J_{\mathrm{Crit}}(x, y, t = 0)$ gets $\Phi(t)$ close to zero if $J_{\mathrm{Crit}}(x, y, t)$ is close to $J_{\mathrm{Crit}}(x, y, t = 0)$, in other words, if the temperature field is not seriously disturbed from its initial values (temperature of coolants). In this case, almost the whole conductor cross section remains open, with high critical current density, to zero loss transport current. However, if $T(x, y, t)$ becomes close to T_{Crit}, $J_{\mathrm{Crit}}(x, y, t)$ is very small at these positions, and $\Phi(t) \to 1$; zero loss current transport current flow then is hardly possible (in a magnetic field, flux flow resistance would come up first). If $T(x, y, t) > T_{\mathrm{Crit}}$, we are finally in the Ohmic resistance regime, in these elements.

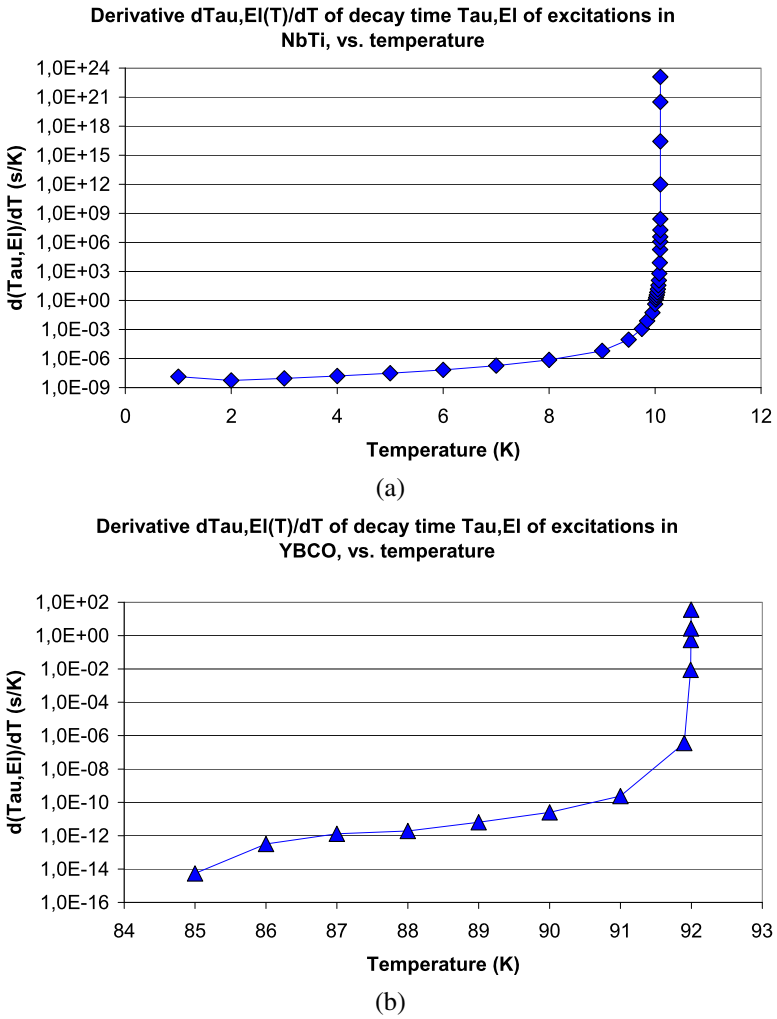

Fig. 8 (**a**) Derivative $d\tau_{\mathrm{El}}/dT$ of the time constant, τ_{El}, with T the element temperature, for decay of thermally excited electrons states in the virtual volume, V_C, of the NbTi filament. (**b**) Derivative $d\tau_{\mathrm{El}}/dT$ of the time constant, τ_{El}, for the YBaCuO filament. Same calculation as in (**a**) (Color figure online)

Accordingly, there could be "mixtures" comprising, in the conductor cross section, regions of zero loss transport current, regions of flux flow resistance, and regions of Ohmic resistance.

In order to determine whether a particular conductor cross section meets the stability criterion expressed by Eq. (16), the stability function $\Phi(t)$ has to be determined, in principle for all axial distances, but it might be sufficient for stability analysis to consider only the maximum of $\Phi(t)$ obtained for all planes, as suggested in [3].

Figure 10 shows $\Phi(t)$ at four axial distances (planes) for the NbTi filament. Position of the planes is identified as follows: plane 1: $y = 0$, plane 2: $y = 18.75$, plane 3: $y = 37.5$, plane 4: $y = 56.3$ μm. Because rather small thermal disturbances have been assumed, the magnitude of the $\Phi(t)$ curves is below 0.3. But the deviation in zero loss transport current (Fig. 11),

$$I_{\mathrm{Transp}}(t) = J_{\mathrm{Crit}}(x, y, 4\ \mathrm{K})\big[1 - \Phi(t)\big], \tag{17}$$

in the four planes and between $10^{-6} \leq t \leq 10^{-4}$ s yet becomes significant.

So far the results for $\Phi(t)$ in the NbTi filament when they are plotted vs. real time, t. Corresponding results for $\Phi(t)$ and $I_{\mathrm{Transp}}(t)$ for the YBCO filament are similar to the results reported in [5] for HTSC pellets and need not be repeated here.

5.2 Stability Function in the Timescale t'

For a plot of the stability function vs. time, t', we now calculate the quantities $\Delta t'$ from Eq. (15) for both samples. It is expected that the correction $\Delta t'$ to real time, t, could perhaps be strong at positions where temperature approaches T_{Crit}. This is confirmed in Fig. 12a, b that shows a plot of shifted time, t', vs. real time, t. For the NbTi filament, a strong peak is observed near the position ($x = 0$, $y = 0$). In case of the YBaCuO filament, there is also a sharp peak, but its magnitude is much smaller, so that we can as before plot the stability function vs. real time, t. In the NbTi fil-

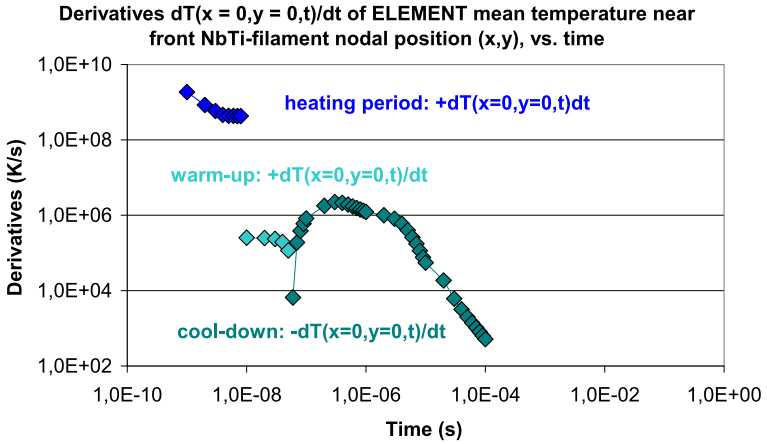

(a)

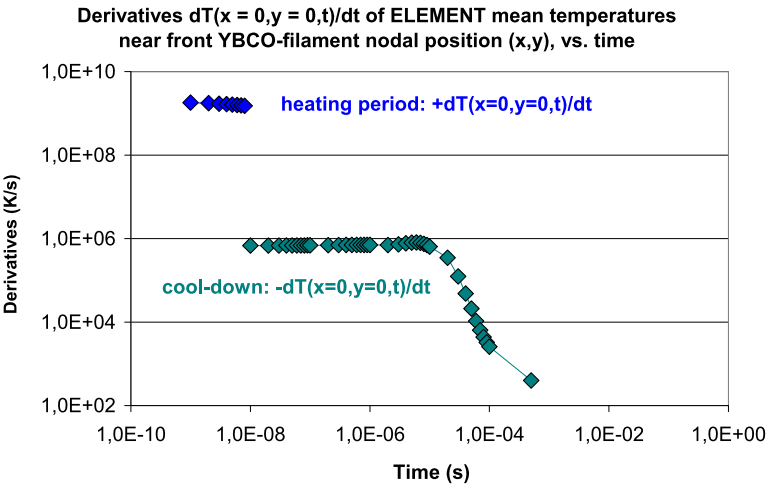

(b)

Fig. 9 (**a**) Derivative dT/dt of element temperature, T, calculated for elements located near front positions of the NbTi filament under a heat pulse absorbed at radial positions $0 \le x \le 6$ μm, $y = 0$, of $Q = 2.5 \times 10^{-10}$ W s during a period of 8 ns. The figure shows dT/dt during heating, warm-up (after end of the heat pulse), and cool-down periods (note the *minus sign*). The warm-up period results from redistribution of heat delivered from the nodes of the concerned finite element and its neighbors. (**b**) Derivative dT/dt of element temperature, T, near front positions of the YBaCuO filament under a heat pulse absorbed at radial positions $0 \le x \le 6$ μm, $y = 0$, of $Q = 3 \times 10^{-8}$ W s during a period of 8 ns. The figure shows dT/dt during heating and cool-down periods (no intermediate warm-up period is observed) (Color figure online)

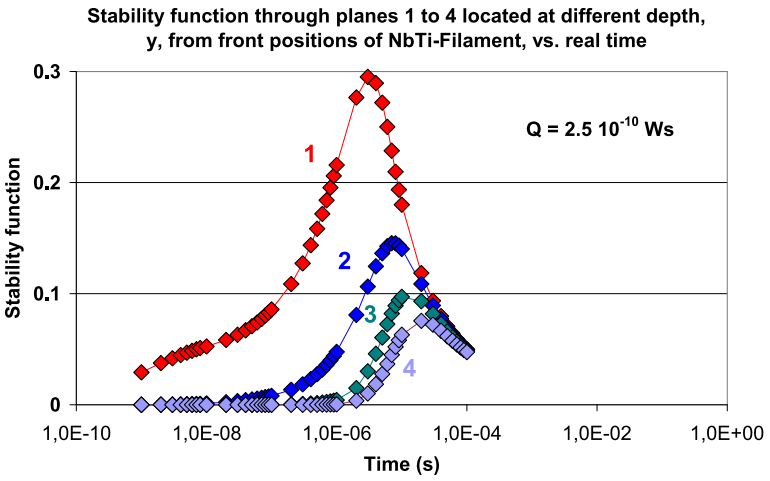

Fig. 10 Stability function, $\Phi(t)$, of the NbTi filament, calculated using Eq. (16) under a heat pulse absorbed at radial positions $0 \le x \le 6$ μm, $y = 0$, of $Q = 2.5 \times 10^{-10}$ W s during a period of 8 ns. The figure shows $\Phi(t)$ at planes 1 to 4 (axial distances from the target spot) of $y = 0$, 18.75, 37.5, and 56.3 μm, respectively (Color figure online)

ament, however, the shifted time, t', locally differs strongly from real time so that critical current density and, as a result, also the stability function, if plotted against shifted time, t', will strongly be different from the corresponding standard plots of $J_{\mathrm{Crit}}(x, y, t)$ and $\Phi(t)$. The magnitudes of $\Phi(t)$ are shifted on the time axis to the proper times, t'.

Figure 13a, b shows critical current density plotted vs. real time (t, solid symbols) and shifted time (t', open sym-

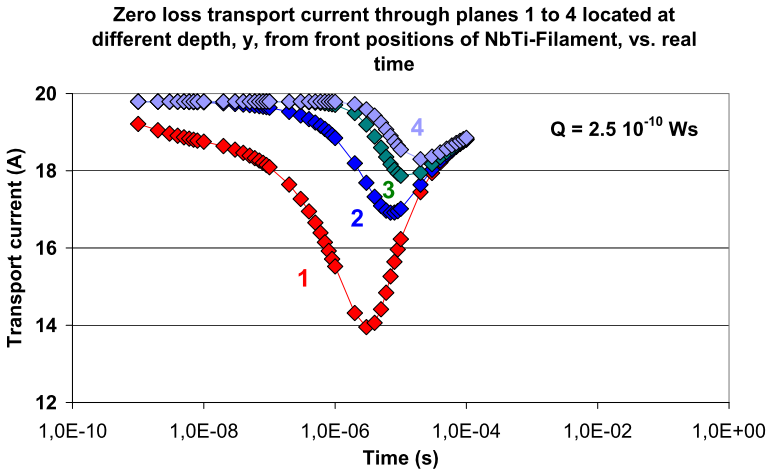

Fig. 11 Zero loss transport current, I, in the NbTi filament calculated using Eq. (17) under a heat pulse absorbed at radial positions $0 \leq x \leq 6$ μm, $y = 0$, of $Q = 2.5 \times 10^{-10}$ W s during a period of 8 ns. The figure shows I at planes 1 to 4 (axial distances from the target spot) of $y = 0$, 18.75, 37.5, and 56.3 μm, respectively (Color figure online)

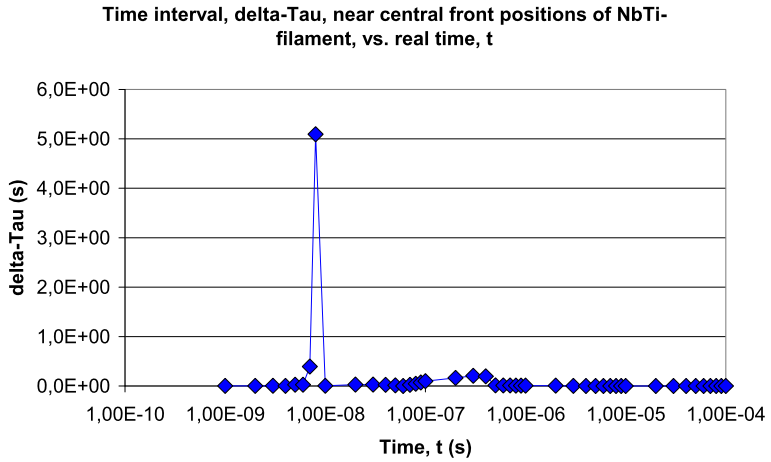

(a)

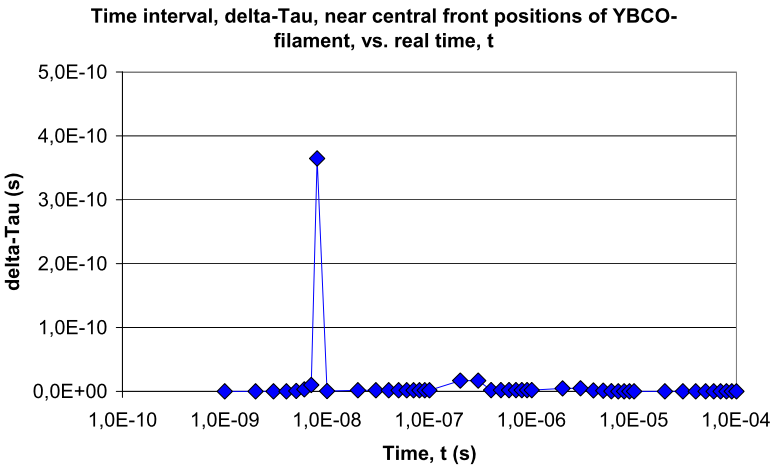

(b)

Fig. 12 (**a**) Time interval, $\Delta\tau_{\mathrm{El}}$, as a function of time, t, calculated in the NbTi filament for the element (in the finite element scheme, Fig. 4) positioned near the central front node ($x = 0$, $y = 0$). See text for more explanations. (**b**) Time interval, $\Delta\tau_{\mathrm{El}}$, in the superconducting YBaCuO filament. Same calculation as in (**a**). See text for more explanations (Color figure online)

bols). For the NbTi material, the deviation is strong since the time shift, at position $(x = 0, y = 0)$, reaches values up to 5 s. But in the YBaCuO filament, the deviation between the curves $J_{\mathrm{Crit}}(x = 0, y = 0, t)$ and $J_{\mathrm{Crit}}(x = 0, y = 0, t')$ is very small, as was to be expected.

A corresponding behavior has to be expected for the stability function. In case of the YBaCuO filament, there will be hardly any difference between $\Phi(t)$ and $\Phi(t')$, but with the NbTi filament, the deviation may be significant. It is exactly for this reason that a problem comes up.

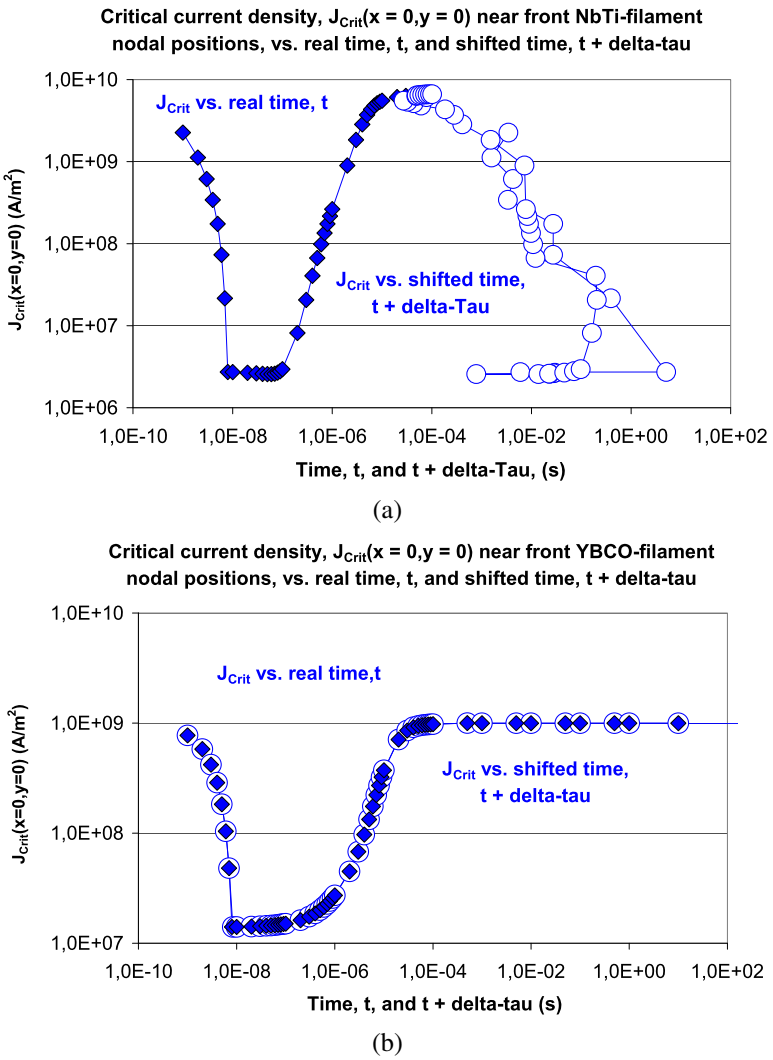

Fig. 13 (**a**) Critical current density in the superconducting NbTi filament. Data are calculated from the element temperatures reported in Fig. 6a using Eq. (14) with the exponent $n = 3/2$ and are given for the element (of the finite element scheme, Fig. 4) positioned near the central node ($x = 0$, $y = 0$). The *solid symbols* are the same as in Fig. 7a. Data $J_{\mathrm{Crit}}(x, y, t)$ are plotted vs. real time scale t (*solid symbols*) and the "shifted" time scale $t' = t + \Delta\tau_{\mathrm{El}}$ (*open symbols*), with the shift $\Delta\tau_{\mathrm{El}}$ from Fig. 12a. See text for more explanations. (**b**) Critical current density in the superconducting YBaCuO filament. Data are calculated from the element temperatures reported in Fig. 6b using Eq. (14) with the exponent $n = 2$ and are given for the element (of the finite element scheme, Fig. 4) positioned near the central node ($x = 0$, $y = 0$). The *solid symbols* are the same as in Fig. 7b. Data $J_{\mathrm{Crit}}(x, y, t)$ are plotted vs. real time scale t (*solid symbols*) and the "shifted" time scale $t' = t + \Delta\tau_{\mathrm{El}}$ (*open symbols*), with the shift $\Delta\tau_{\mathrm{El}}$ from Fig. 12b. See text for more explanations (Color figure online)

Corrections $\Delta t' = \Delta t'(x, y, t) = \tau_{\mathrm{El}}(x, y, t)$ and shifted times $t' = t'(x, y, t) = t + \tau_{\mathrm{El}}(x, y, t)$ are different in each element (i.e., at each arbitrary position x, y in the conductor) because the temperature field $T(x, y, t)$ is different in each element, and so is $\tau_{\mathrm{El}}(x, y, t)$. It is therefore not possible to define a unique shifted time, t', that would exactly be the same for *all* elements in any plane located close to the target spot. This excludes the usual plot of the stability function, $\Phi(t)$, in dependence of one and only one, uniquely defined time, at positions near the disturbance.

This problem becomes the weaker the larger the axial distance of the planes y from the target spot. This is demonstrated in Fig. 14: if we tentatively calculate the arithmetic mean of $\Phi(x, y, t')$ taken over all elements in a single plane y, then the curves $\Phi(x, y, t')$ approach the standard $\Phi(x, y, t)$ the more the larger the axial distance, y, from the target spot.

Stability analysis accordingly should be performed not at exactly the position $y = 0$ where the disturbance is located or at distances close to this position. Instead, the analysis should observe appropriate, safety-related distances. These distances are correlated to propagation of the corresponding temperature field. For the NbTi filament, the minimum distance to be observed, at the given conditions, is at least 60 μm, while it is near zero in case of the YBaCuO filament. It is clear that the minimum distance depends on the evolution of the particular temperature field, i.e., on the geometrical and thermal parameters (radius and material of filament and matrix, boundary conditions, diffusivity, location and magnitude of heat pulse, and others). The minimum distances thus may become larger if the temperature field looks different, e.g., under strong thermal disturbances (note that the disturbances, Q, in the two filaments were chosen not to increase transient temperature above T_{Crit}).

Another consequence from the different timescales, t and t', not only affects the stability function. In a step before, it might directly concern critical current density: if under a disturbance the electron system is thermally excited, which

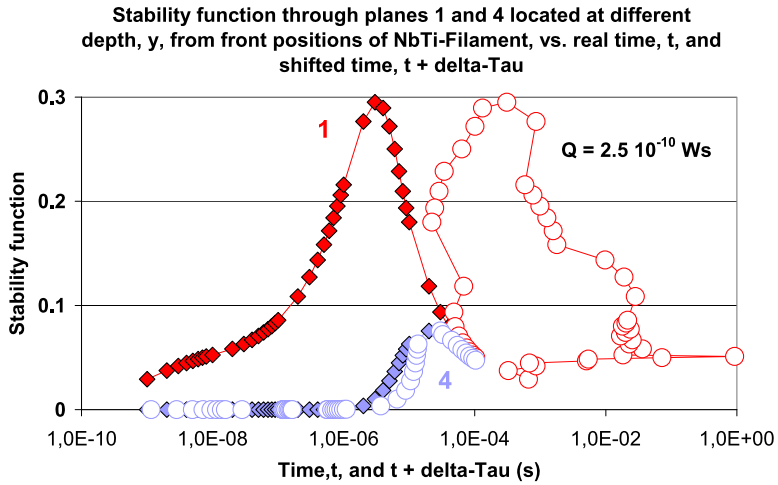

Fig. 14 Stability function, $\Phi(t)$, of the NbTi filament, calculated using Eq. (16) under a heat pulse absorbed at radial positions $0 \le x \le 6$ μm, $y = 0$, of $Q = 2.5 \times 10^{-10}$ W s during a period of 8 ns. The figure shows $\Phi(t)$ at planes 1 and 4 (axial distances from the target spot) of $y = 0$ and 56.3 μm, respectively. The *solid symbols* are the same as in Fig. 10. Data $\Phi(t)$ are plotted vs. real time scale t (*solid symbols*) and the "shifted" time scale $t' = t + \Delta\tau_{\mathrm{El}}$ (*open symbols*), as a rough approximation with an arithmetic mean $\Delta\tau_{\mathrm{El}}$ of the shift $\Delta\tau_{\mathrm{El}}(x, y, t)$ taken over the corresponding planes. See text for more explanations (Color figure online)

means that there is a reduction of the density of electron pairs available for zero loss transport current (or in a magnetic field, shielding current), there could be a reduction of the magnitude of critical current density, or if critical current density is conserved, a reduction of the available conductor cross section that is open for zero loss transport. In other words, it is not clear that during the interval $\tau = \tau_{\mathrm{El}}$, a sufficiently large number of electron pairs would (already?) be available. Consequences for a technical application, possibly arising from this observation, will be discussed in the next section.

6 Consequences for Safe Operation of a Resistive Fault Current Limiter

A current limiter shall respond, within very short periods of time, to a disturbance (short circuit, lightning), and clearly below 50 ms (for stable operation conditions, a difficult task) create an electrical resistance large enough to limit the fault current to values prescribed by safety aspects of the electrical circuit to be protected. The question is: which magnitude of critical current density (before start of the disturbance) is at least required to successfully operate a resistive current limiter if an appropriate superconductor material (generating no hot spots over extended conductor length) is available?

In the following, for simplicity, we assume adiabatic conditions. This assumption is justified because it usually takes the thermal wave, generated under fault current by the increasing electrical resistance, considerably more time (several 10 ms, even under a large fault current) to arrive at the conductor periphery, where it could induce pool boiling, much longer than it takes the conductor to enter a highly resistive state. Heat transfer to the coolant by conduction and convection that would be created earlier than pool boiling can be neglected, within these time intervals (the corresponding heat transfer rate are by orders of magnitude smaller than for pool boiling). Accordingly, the conductor, due to the fault current, is already in a resistive state.

Assuming a maximum tolerable fault current density, $J_{\max}$, the resistive heat loss per unit conductor volume, V, from this current amounts to

$$(dQ/dt)/V = \rho_{\mathrm{El}} J_{\max}^2 \tag{18a}$$

with ρ_{El} the specific electrical resistance of the conductor. We replace the derivative $(dQ/dt)/V$ by the ratio of finite differences, $(\Delta Q/\Delta t)/V$, where $\Delta Q = \rho c_p \Delta T$ is the heat generated within the reaction period, Δt, of the limiter (the triggering time detected when the conductor finally arrives at large Ohmic electrical resistance). In this expression, ρ and c_p denote the density and specific heat of the conductor material. Again for simplicity, we assume that both quantities ρ and c_p are independent of temperature (in any real application, this assumption would have to be checked carefully). We now expand the right side of this equation as

$$(\Delta Q/\Delta t)/V = J_{\mathrm{Crit}}^2 (\rho c_p \Delta T/\Delta t)/\left(V J_{\mathrm{Crit}}^2\right), \tag{18b}$$

which finally, from comparison with Eq. (18a), yields

$$M = J_{\max}/J_{\mathrm{Crit}} = K/J_{\mathrm{Crit}} \tag{18c}$$

with a constant $K = [(\rho c_p/\rho_{El})(\Delta T/\Delta t)]^{1/2}$. Accordingly, if the electric circuit to be protected can tolerate a maximum fault current density J_{max} that is a multiple M of J_{Crit}, then this multiple depends inversely on J_{Crit}. In order to safely protect the circuit, M should be as small as possible. Medium voltage transformers usually cannot steadily stand multiples M larger than 1.5. Small M can be achieved, within these approximations, if J_{Crit} is large, assuming that the constant K really is constant and does not depend too strongly on temperature (via the materials parameters) and not too strongly, and directly, on the excursion $(\Delta T/\Delta t)$.

Relation (18c) has successfully been confirmed in experiments with Bi2223-conductor by Abeln et al. [19].

It is clear that safety of the electric circuit would dangerously be affected if J_{Crit} would temporarily become small during a "dead time" interval $\Delta\tau_{El}$.

7 Summary and Conclusions

We have studied the impact of decay of excited electron states on superconductor stability. A sequential model has been presented to estimate the time, τ, needed for return of the disturbed electron system of a superconductor to a new dynamic equilibrium. Average decay rates of the excited electron system were estimated using a time-of-flight concept (the process of exchanging information between two quantum states by a mediating Boson). From the obtained numerical results, the period of time (relaxation time), $\tau = \tau_{El}$, needed to rearrange the total wave function to a new dynamic equilibrium has been calculated. These results cannot be obtained in solely particle-related experiments like current injection where conservation of charge, mass, etc. are in the foreground.

From the preceding analysis it has to be expected that temporal mismatch between relaxation times τ_{Ph} and τ_{El} creates different timescales, t and t', of which the scale t' is not a constant but is different in different regions of the superconductor. The effect could be strong at temperatures near conductor phase transition. Besides the magnitude of critical current density and stability function, this difference could affect also measurement of observables like levitation of a superconductor in a magnetic field or results of the electronic part of the specific heat measurements, i.e., in all experiments where critical current density is concerned in any way. As an example, the possibly existing effect has been discussed for operation of a fault current limiter. A decrease of critical current density due to a "dead time interval" during which only a reduced number of electron pairs would be available for zero loss current transport could dangerously affect safe operation of the limiter and the electrical circuit to be protected.

Appendix A: Decay in Space, Lifetime from a Diffusion Model Approach (Supplement to Sect. 3.1)

Because of its finite thermal diffusivity, nonequilibrium thermal states, during warm-up or cool-down periods, always arise *locally* in a superconductor, from local temperature gradients, from different thermal boundary conditions, or from internal heat sources. Temperature evolution in real solid samples never develops perfectly uniformly.

The situation in superconductors when exposed to absorption of a heat pulse is analogous to standard laser flash experiments in which at a time t_0 a very short radiation pulse is directed onto a thin film sample. Assume that the sample initially is at uniform temperature. Absorption of the pulse locally increases sample front surface temperature to a maximum obtained at a time $t_1 > t_0$ that is overlaid onto the previous uniform temperature (background) level. The laser flash experiment then involves observation of front or rear surface temperature to obtain the thermal diffusivity of the sample material; in the most simple procedure, the diffusivity is obtained at a time, $t_{1/2}$, when rear surface temperature has increased to half its maximum value.

Determination of the lifetime of thermally excited states of superconductors, the diffusion aspect (or decay of the excitation in space) is modeled in the following in a quite analogous way, with the exception that we do not look for the time $t_{1/2}$ when the concentration of surplus excited states has decayed to half its initial value after end of the disturbance. Instead, we look for the time t_∞ when the disturbance (the concentration of excited electron states) has decayed completely, $c(\mathbf{x}, t_\infty) = \text{const}$. This concept has successfully been applied in [20], where an instantaneous, internal pulse method was used in an exotic material.

In the tunnel (current injection) experiment described in Fig. 3 of [9], delivery of a short *electrical current* pulse to the active contact area of the upper film (the source being a very small volume, V_J, about 10^{-24} m^3) causes the previous dynamic equilibrium concentration of electron excitations to increase to transient values. These excitations decay according to electrical conduction properties of the tunnel junction into electronic states that can be occupied in the lower film and by loss of phonons that cannot contribute to reabsorption/generation of new quasi-particles.

Delivery of a short *heat* pulse, e.g., from a laser directed onto the surface of a thin film or of a pellet, with the heat pulse absorbed in a small volume, $V_{th} \gg V_J$, near the surface that is part of the total volume, V, of the sample causes local temperature in V_{th} to increase above equilibrium (start) temperature. As a consequence, there is propagation of (a) a thermal wave and (b) of a concentration wave of excited electron states from V_{th}, because of thermal conductive properties of the solid material and because of a concentration gradient, respectively. It is tempting to assume that not

only propagation of the thermal wave but also redistribution of the concentration of excited electron states can be described as a diffusion process.

These two decay channels have to be distinguished as follows:

(i) Propagation of the thermal wave from V_{th} into the solid increases temperature over local start values, $T = T(\mathbf{x}, t_0)$. This also initiates increase of concentration of excited states, at the same positions outside V_{th}, over local start values, $c = c(\mathbf{x}, t_0)$, because of coupling between temperature and temperature-dependent density of excitations (there are accordingly "source terms" initiated by the temperature field for increase of concentration).

(ii) Propagation of the concentration wave from V_{th} into the solid increases the concentration of excitations over local start values, $c = c(\mathbf{x}, t_0)$, now merely by diffusion under a concentration gradient but without source terms (source and sink terms, if any, would cancel each other).

This means that there is a diffusion "front" of the concentration of excitations driven by two different mechanisms, one of which is closely coupled to propagation of the thermal wave. Both mechanisms, propagation of a diffusion front of concentrations and of a thermal wave, penetrate in parallel into the solid material, but with different speed.

With this separation, de-excitation of the over-concentration of excited electron states in V_{th} originating from absorption of the heat pulse can be described by evolution of the total wave function $\psi(\mathbf{x}, t)$: if $\mathbf{x} = \mathbf{x}(t)$ indicates the diffusion front of the order parameter, $c = |\psi(\mathbf{x}, t)|^2$, we have, in one dimension, the expression (given already in Eq. (4))

$$dc(\mathbf{x}, t)/dt = \big(\partial c(\mathbf{x}, t)/\partial x\big)(\partial x/\partial t) + \partial c(\mathbf{x}, t)/\partial t. \qquad (19)$$

The first factor in Eq. (19), the concentration gradient $\partial c(\mathbf{x}, t)/\partial x$, describes de-excitation (decay of the disturbance) by diffusion (or decay "in space"), the second factor, $\partial x/\partial t$, the speed at which the diffusion front propagates, and the term $\partial c(\mathbf{x}, t)/\partial t$ indicates the decay "in time" of the disturbance. The first contribution, $(\partial c(\mathbf{x}, t)/\partial x)(\partial x/\partial t)$, accordingly comprises channels (i) and (ii) mentioned above that both will be modeled using diffusion methods. The contribution $\partial c(\mathbf{x}, t)/\partial t$ is investigated in Sects. 3 to 5 of the present paper.

An analogue to "decay in space" is an expanding cloud of radioactive particles. In this picture, "decay in time" concerns decay rates following from classical exponential decay law. In comparison with the present case, excited electron states and electron pairs are the analogues of mother and daughter terms, respectively.

Since superconductor solids are opaque, radiation from the laser source (the incident heat pulse) will penetrate to only a very small distance, d_{Rad}, into the solid volume. Together with the diameter of the target spot, this defines a source volume. For simplicity, we will assume that the sample is kept at adiabatic conditions, at least during a time interval that is long compared to the lifetime of the disturbance.

For modeling the propagation of excited electron states in the solid by diffusion, i.e., the decay channel (ii) of the above, the following questions have to be answered:

(1) Which kind of interaction is observed that in a diffusion manner (if any) has to proceed stepwise?
(2) How large is the mean free path, in relation to sample dimensions, between two such interactions?
(3) How fast will the interaction propagate into the sample, in particular compared to the thermal wave?
(4) Is it possible to assign a diffusivity to the propagation of the interaction?

At positions $\mathbf{x}$ inside the source volume, V_{th}, and during decay of the disturbance, the order parameter increases with time because the number of excitations decreases. Outside this volume, under solely thermal conduction condition, the order parameter decreases (distribution of the thermal disturbance at these positions leads to local increase of the number of excitations). It is thus the order parameter that diffuses within the solid volume. What then is the driving mechanism that would cause the order parameter to diffuse?

Consider inside the source volume, V_{th}, a number of N excited electron states that result from previous decay of $N/2$ electron pairs in the same volume. The excited states, or concentrations thereof, can be assigned an enthalpy, g_{Exc}, that is larger than the corresponding enthalpy, g_{EP}, of electron pairs, and it is the enthalpy difference that drives excited states to recombine to electron pairs (consistent with temperature evolution in this volume).

Ohm's law for transport of electrical current of density, $\mathbf{J}$, under an electrical field, $\mathbf{E}$, is a classical diffusion law: in metals, $\mathbf{J} = [(ne^2\tau)/2m]\mathbf{E}$ (with n the concentration of electrons, e and m the unit electrical charge and mass of electrons, and here τ the time of flight between two scattering events). The electrons under the electrical field move with the drift velocity, $\mathbf{v}_D = -e\mathbf{E}\tau/(2m)$, in Cu at RT with a mean free path of only about 5 nm. A simple expression like Ohm's diffusion law of the movement of single charge carriers (electrons) is distinct from correlation between pairs: a current density $\mathbf{J} > 0$ exists only if the coherent state of *all* electron pairs moves with a common, nonzero center-of-mass velocity. Neither is it possible to define a mean free path of *one* electron pair nor of a cloud of all coherently coupled pairs. Therefore, the main precondition for a diffusion approach, drift of *individuals* (or of a cloud), under a potential difference and with interactions imposed by obstacles, for both species is not available in a superconductor.

This problem can be removed if we consider propagation of *concentrations* of pairs and of excitations. In this case, it is no longer necessary to specify the behavior of individuals, and the mean free path can be defined with respect to decrease of concentration over a path the length of which can be estimated from exponential decay of the concentration, as in radiative heat transfer where the mean free path indicates exponential decay of the radiation intensity, not of a single but of multiple photons, on the statistical average. The mean free path of the concentration of excited electron states under diffusion is given by the Ginzburg–Landau (GL) coherence length, ξ_{GL}. With ξ_{GL} in the order of 1 nm in YBaCuO, this is very small in comparison to sample dimension, which means that the precondition for "diffusion" to be a stepwise process would be fulfilled.

The velocity by which the diffusion propagates can be approximated by the phonon velocity, v_{Ph}, because v_{Ph} is the velocity of the Boson that mediates the binding interaction between two electrons. As a rough estimate, we take a value v_{Ph} of about 1/100 of the Fermi velocity (the latter describes the velocity of electron pairs carrying a supercurrent).

Calculation of the evolution with time of the *concentration*, $c_{\mathrm{Exc}}(t)$, of excited states propagating by the two above-mentioned channels (i) and (ii) then is performed by use of Fourier's differential equation. For description of $c_{\mathrm{Exc}}(t)$, again in one dimension, we have

$$\partial c/\partial t = D_c \partial^2 c(t)/\partial x^2 \quad \text{with Source terms} \tag{20}$$

at all times $t > t_1$ where t_1 indicates the end of the thermal disturbance (approximately the duration of the heat pulse). For description of the temperature evolution, we have

$$\partial T/\partial t = D_{\mathrm{th}} \partial^2 T(t)/\partial x^2 \quad \text{without Source terms.} \tag{21}$$

Both Eqs. (6a) and (6b) are coupled by temperature dependence of the concentration $c_{\mathrm{Exc}}(t)$, see below.

The thermal diffusivity, $D_{\mathrm{th}} = D_{\mathrm{th}}(T)$, in Eq. (21) is calculated from temperature-dependent values of conductivity, specific heat and density of YBaCuO applied already in [5] and the other publications of the author as cited in the text.

The concentration diffusivity, D_c, in Eq. (22) in analogy to thermal transport, can, probably only very roughly, be determined from

$$D_c = (1+\delta)(5/2) v_{\mathrm{Ph}} \xi_{\mathrm{GL}} \tag{22}$$

(see Kennard [21], Chap. 4, Sect. 102, and references cited therein). Equation (22) applies the conductivity of a two-atomic gas in the hard core approximation. The quantity δ is small, in the order of 1/100. Numerical values of D_c, for v_{Ph} constant at about 9.4×10^3 m/s, and in a broad interval $0.1 \le \xi_{\mathrm{GL}} \le 10$ nm are between 7.9×10^{-7} and 7.9×10^{-5} m^2/s. For $\xi_{\mathrm{GL}} = 3$ nm, D_c is about one order of magnitude below the diffusivity (2.5×10^{-4} m^2/s) reported in Loidl et al. [22] for quasi-particle diffusion in a W/Al bi-layer diffusion film. Such a decrease of the diffusivity is qualitatively to be expected for a high-temperature superconductor.

The source terms in Eq. (20) arise from the temperature dependence of $c_{\mathrm{Exc}}(T)$ and its coupling to the temperature field. These terms describe excitations at positions, $\mathbf{x}$, within the total volume as soon as the thermal wave arrives at these positions. For simplicity, we use the equilibrium expression for the temperature dependence of the concentration. In a time interval dt, we have

$$(dc_{\mathrm{Exc}}/dT)(dT/dt)dt = c_{\mathrm{Exc},0} \exp\left[-\Delta E(T)/(kT)\right] dt \tag{23}$$

with binding energy, ΔE, taken as temperature dependent using for simplicity the BSC-result

$$\Delta E(T) = 1.74 \Delta E(T=0) \times (1-\gamma)^{1/2} \tag{24}$$

indicated in Blatt [14], p. 243. In Eqs. (23), (24), $c_{\mathrm{Exc},0} = 6 \times 10^{26}$ 1/m^3, $\Delta E(T=0) = 60$ meV for high-temperature superconductors, and $\gamma = T/T_{\mathrm{crit}}$. Equation (24) results from an exact thermo-dynamical solution at nonzero temperature provided by the theory of Bogoliubov, Zubarev, and Tserkovnikov (as Blatt [14], p. 227, points out, one of the very few exact theories in statistical mechanics). The weak point in the present analysis thus results from by Eq. (22) and from Eq. (24) because this equation might not appropriately be applicable to an HTSC material.

In case there are single electrons near the Fermi energy, the Pauli exclusion principle blocks electron states that otherwise could be populated by decay products from pairs, which means that the binding energy of electron pairs, or width of the energy gap, decreases as temperature approaches T_{Crit}. This aspect is reflected by the temperature dependence of ΔE. It also provides an infinite slope of $\Delta E(T)$ at $T = T_{\mathrm{Crit}}$, with a second-order transition, which is consistent with the jump of the electron part of the specific heat at T_{Crit}.

Because of $T = T(x, y, t)$, all quantities γ, ΔE, and dc_{Exc}/dt in Eqs. (23), (24) depend on positions $\mathbf{x} = (x, y)$ and time.

As a result, obtained again from a finite element simulation, the contribution of "decay in space" is much smaller than that obtained for "decay in time". This is the finding for a YBaCuO pellet. The reader interested in more details and numerical results may consult [6].

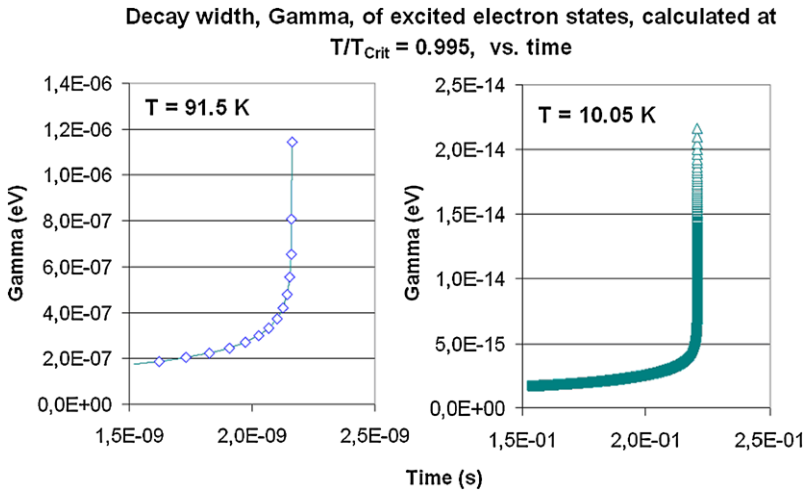

Fig. 15 Decay width, $\Gamma(t)$, of excited electron states, calculated for NbTi (*right*) and YBaCuO-filaments (*left part of the figure*) for the same ratio, $T/T_{\mathrm{Crit}} = 0.995$, of momentary temperature, $T(t)$, to critical temperature of the superconductors (10.1 and 92 K, for NbTi and YBaCuO, respectively)

Appendix B: Comparison with Classical Exponential Decay Formula

Comparison of decay widths, $\Gamma(t)$, for NbTi and YBaCuO-filaments demonstrates the enormous differences in decay probability, which means YBaCuO will much faster return to dynamical equilibrium than NbTi. This reflects the corresponding higher decay rates of YBaCuO given in Fig. 3b which in turn are the consequence of the much higher operating temperature of this superconductor.

References

1. Wilson, M.N.: Superconducting magnets. In: Scurlock, R.G. (ed.) Monographs on Cryogenics. Oxford University Press, New York (1989). Reprinted paperback
2. Dresner, L.: Stability of superconductors. In: Wolf, St. (ed.) Selected Topics in Superconductivity. Plenum, New York (1995)
3. Flik, M.L., Tien, C.L.: Intrinsic thermal stability of anisotropic thin-film superconductors. In: ASME Winter Ann. Meeting, Chikago, IL, Nov 29–Dec 2 (1988)
4. Reiss, H.: An approach to the dynamic stability of high-temperature superconductors. High Temp., High Press. **25**, 135–159 (1993)
5. Reiss, H.: Radiation heat transfer and its impact on stability against quench of a superconductor. J. Supercond. Nov. Magn. **25**(2), 339–350 (2012)
6. Reiss, H.: Impact of lifetime and decay rates of thermally excited states in superconductors on a gravity experiment. In: Modanese, G., Robertson, G.A. (eds.) Gravity-Superconductor Interaction: Theory and Experiment 2011, pp. 288–324. Bentham Science, London (2012)
7. Mattuck, R.D.: A Guide to Feynman Diagrams in the Many-Body Problem. McGraw-Hill, Maidenhead (1967)
8. Gray, K.E.: Steady state measurement of the quasiparticle lifetime in superconducting aluminium. J. Phys. F, Met. Phys. **1**, 290–308 (1971)
9. Epperlein, P.W., Lassmann, K., Eisenmenger, W.: Quasiparticle recombination time in superconducting tin and normal electron density of states at the Fermi surface from tunnel junction experiments. Z. Phys. B **31**, 377–384 (1978)
10. Carslaw, H.S., Jaeger, J.C.: Conduction of Heat in Solids, 2nd edn. Clarendon, Oxford (1959)
11. Hellwege, K.H.: Einführung in die Festkörperphysik, 3rd edn. Springer, Berlin (1988)
12. Mayer-Kuckuk, T.: Kernphysik, Teubner Studienbücher Physik, 4th edn. (1984). Stuttgart, Germany
13. Annett, J.F.: Superconductivity, Superfluids and Condensates, Oxford Master Series in Condensed Matter Physics. Oxford University Press, Oxford (2010). Reprinted edition
14. Blatt, J.M.: Theory of Superconductivity. Academic Press, New York (1964)
15. Pines, D.: Understanding high temperature superconductivity: progress and prospects, Manuscript Director's Colloquium, Los Alamos National Laboratory, 1–16 (1997)
16. De Gennes, P.: Superconductivity of Metals and Alloys. Benjamin, New York (1966)
17. Reiss, H., Troitsky, O.Yu.: Radiative transfer and its impact on thermal diffusivity determined in remote sensing. In: Reimer, A. (ed.) Horizons in World Physics, vol. 276, pp. 1–68 (2011). Open access paper
18. Reiss, H., Troitsky, O.Yu.: The Meissner–Ochsenfeld effect as a possible tool to control anisotropy of thermal conductivity and pinning strength of type II superconductors. Cryogenics **49**, 433–448 (2009)
19. Abeln, A.: ABB Corporate Research Centre, Heidelberg, Germany, in: Entwicklung von wechselstromtauglichen Supraleitern mit hohen Übergangstemperaturen für die Energietechnik, Part C: Anwendungsbezogene Arbeiten, Final report to Bundesministerium für Forschung und Technologie, Bonn, Germany, Forschungsvorhaben 13 N 5610 A (1994)
20. Reiss, H., Troitsky, O.Yu.: A thermophysical model to numerically determine the diffusivity of highly excited nuclear matter with an instantaneous, internal pulse method. J. Chem. Eng. Data **54**(9), 2483–2497 (2009). William. A. Wakeham Festschrift
21. Kennard, E.H.: Kinetic Theory of Gases. McGraw-Hill, New York (1938)
22. Loidl, M., Cooper, S., Meier, O., Pröbst, F., Sáfrán, G., Seidel, W., Sisti, M., Stodolsky, L., Uchaikin, S.: Quasiparticle diffusion over several mm in cryogenic detectors. Nucl. Instrum. Methods Phys. Res., Sect. A **465**(2–3), 440–446 (2001)